

C.2

NACA RM E56C08

**NACA**

# RESEARCH MEMORANDUM

ANALYTICAL AND EXPERIMENTAL INVESTIGATION OF A  
TEMPERATURE-SCHEDULE ACCELERATION CONTROL  
FOR A TURBOJET ENGINE

By Herbert Heppler, Paul M. Stiglic, and David Novik

Lewis Flight Propulsion Laboratory  
Cleveland, Ohio

CLASSIFICATION CHANGED

UNCLASSIFIED

To

By authority of TPA #33 Data 10-28-60  
ERB

CLASSIFIED DOCUMENT

This material contains information affecting the National Defense of the United States within the meaning of the espionage laws, Title 18, U.S.C., Secs. 793 and 794, the transmission or revelation of which in any manner to an unauthorized person is prohibited by law.

## NATIONAL ADVISORY COMMITTEE FOR AERONAUTICS

WASHINGTON

June 22, 1956

**CONFIDENTIAL**

UNCLASSIFIED

## NATIONAL ADVISORY COMMITTEE FOR AERONAUTICS

RESEARCH MEMORANDUMANALYTICAL AND EXPERIMENTAL INVESTIGATION OF A TEMPERATURE-  
SCHEDULE ACCELERATION CONTROL FOR A TURBOJET ENGINE

By Herbert Heppler, Paul M. Stiglic, and David Novik

## SUMMARY

A temperature-limiting control was used on a turbojet engine in order to study the feasibility of its use as an acceleration control. Three types of control action, proportional, integral, and proportional-plus-integral, were used in this investigation.

Transient response data were obtained to investigate the control-system response and stability. Temperature errors, which include overshoot, tracking, and steady-state errors combined with control stability, were used as control criteria to evaluate the control systems.

The most favorable of the control systems tested was found to be the proportional-plus-integral control action, which had no steady-state error, a negligible tracking error, minimum temperature overshoot, and was stable to a higher control gain.

## INTRODUCTION

One of the main objectives in controlling a turbojet engine is to provide for rapid, safe accelerations from one thrust level to another. Maximum acceleration has been found to occur at the compressor stall line as shown in reference 1. Since acceleration diminishes or may be impossible in the stall region, it is desirable to accelerate with a safe margin from the stall line.

Two general turbojet acceleration control systems have been investigated at the NACA Lewis laboratory. One utilizes the optimizing technique which requires an engine parameter signal to warn of impending stall. This method may be desirable because maximum acceleration could be safely attained independent of altitude corrections and engine deterioration. However, a preliminary investigation (ref. 2) to search for adequate stall-warning signals proved unsuccessful. No applicable

UNCLASSIFIED

control signals were found. Until an adequate stall-warning signal is found, other types of acceleration controls must therefore be used.

The second type of control automatically limits engine parameters such as fuel flow, acceleration, compressor discharge pressure, or temperature according to a predetermined schedule. An investigation of scheduling engine acceleration with engine speed is presented in reference 3.

This report investigates some of the problems involved in scheduling the tailpipe temperature to avoid stall during acceleration. A major difficulty in using the tailpipe temperature as a control parameter is the development of a suitable temperature-sensing device. In order to maintain a safe margin between surge and scheduled values, accurate temperature measurements are needed. A compensating device was used to cancel the large thermocouple lag associated with heavy long-life thermocouples usually necessary for high-temperature measurement.

The object of this report is to investigate the dynamics of a closed-loop acceleration control that follows a schedule of tailpipe temperature with rotor speed. Acceleration is limited by one of two factors, engine surge or turbine temperature. A constant temperature schedule may be used in a surge- and stall-free region combined with a lower temperature schedule shaped to skirt the surge region. If the engine should inadvertently surge or stall, the resulting overtemperature condition reduces fuel flow to a safe operating value.

The ability of the control to limit temperature overshoot and track the temperature schedule during an acceleration is studied along with the factors influencing the system stability.

## APPARATUS AND INSTRUMENTATION

### Fuel System

The fuel system (fig. 1) consists of a reducing-type differential pressure regulator that maintains a constant pressure drop across the throttle. The response of the throttle valve to input voltage was essentially flat to 20 cycles per second (ref. 4). Because the throttle position was proportional to fuel flow through the throttle, it was used as an indication of fuel flow.

Fuel metered at the throttle flowed to a flow divider which regulates flow to a dual-manifold distribution system as shown in figure 1. The flow divider permitted flow through both the large- and small-slot manifolds at high fuel pressure and to the small-slot manifold at low fuel pressure. The transition from small-slot manifold operation to

both small- and large-slot manifold operation had a capacitive effect on the fuel system. A finite time was necessary to fill the large-slot manifold, which lowered the effective fuel flow for that period. A sudden increase to the required flow occurs when the large-slot nozzle opens. During the short period required to fill the large-slot manifold, throttle position is not a true indication of engine fuel flow.

### Sensors

Tailpipe temperature. - The average of three chromel-alumel thermocouples spaced  $120^{\circ}$  apart was used for tailpipe-temperature measurement. These high-temperature thermocouples were made of 14-gage wire and had an approximate first-order lag that varied with engine speed (fig. 2). The time constant of the thermocouple lag varied from 0.62 second at idle speed to 0.25 second at rated engine speed.

A thermocouple compensator of a lead-lag nature (fig. 3) was used to extend the thermocouple frequency response. The lead time constant was set to cancel the thermocouple lag at 66-percent rated speed. This results in fixed compensator time constants of 0.56-second lead and 0.032-second lag as shown in figure 3.

Since the thermocouple lag decreases with engine speed, the compensator matching at a low engine speed results in overcompensation at higher engine speeds. This overcompensation presents slightly higher peak-temperature measurements than actually exist, resulting in a larger safety margin. A comparison of the compensated and uncompensated thermocouple frequency response with engine speed is shown in figure 4. At 66-percent rated engine speed, the compensated thermocouple is flat to 5 cycles per second, whereas the uncompensated thermocouple response attenuates to 0.055 at 5 cycles per second. As engine speed increases above 66-percent rated speed, overcompensation increases to a maximum of 2.25 at rated speed. The necessity of scheduling exact compensation depends on the accuracy required for the entire control-loop response.

Engine speed. - An electronic counter modified to convert pulses supplied from a 180-tooth tachometer generator into a direct-current voltage was used to obtain engine speed. The direct-current voltage that was proportional to engine speed was filtered and amplified before being recorded.

Engine acceleration. - An acceleration signal was supplied by electronically differentiating the engine speed signal. Filtering of objectionable noise was necessary.

## Recording Equipment

Transient data were recorded on a direct-recording oscillograph, the frequency response of which was essentially flat to 100 cycles per second. A recorder chart speed of 25 millimeters per second was used.

## CONTROL SYSTEM

A block diagram of the control system is shown in figure 5. The demand signal simulates a signal from an operator's throttle, a speed controller, or a temperature controller. This signal sets the desired fuel flow that is metered by the fuel system to the turbojet engine. Tailpipe temperature is measured by the temperature sensor, which also compensates for the instrumentation lag associated with the thermocouple. This compensated temperature signal is compared with the schedule signal, and the error signal is amplified by the control amplifier. The temperature controller begins operating when the error signal indicates an overtemperature. The corrective action of the controller was one of three types: (1) proportional, (2) integral, or (3) proportional-plus-integral. The controller-output signal reduces fuel flow by subtracting from the demand signal.

## Controller Operation

The temperature-summing network, control amplifier, and controller were assembled on an electronic differential analyzer and are shown in schematic form in figure 6. The temperature-schedule signal  $T_s$  is added to the negative of the compensated temperature signal  $-T_m$ , and the resultant temperature error is amplified by the first amplifier. The setting of potentiometer  $P_2$  determines the scheduled temperature level, whereas potentiometer setting  $P_1$  sets the control gain. The value of the amplified temperature error is determined as follows:

$$\left( \frac{R_6}{R_4} T_m - \frac{R_6}{R_5} T_s \right) \frac{1}{P_1} = \frac{K_c}{P_1} (T_m - T_s) = \frac{K_c}{P_1} T_e \quad (1)$$

(All symbols are defined in appendix A.)

The controller amplifier shown in figure 6 has two parallel feedback paths. One path is composed of a diode and a resistor  $R_3$ . The value of resistor  $R_3$  is very small compared with the input resistor  $R_1$ . The second feedback path determines the type of controller corrective action. Connecting both resistor  $R_2$  and condenser  $C_2$  results in a proportional-plus-integral control. Resistor  $R_2$ , by itself, or condenser  $C_2$ , by itself, produces proportional or integral action, respectively.

A negative amplified temperature error  $(K_c/P_1)/T_e$  occurs for operation below the temperature schedule value and results in a positive controller output signal  $W_c$ . The positive signal causes the feedback diode to conduct. The resulting controlled output is shown for proportional-plus-integral control system in the following equation:

$$W_c = \frac{-R_3}{R_1} \left( \frac{1 + R_2 C_2 s}{1 + R_2 C_2 s + R_3 C_2 s} \right) \left( \frac{-T_e K_c}{P_1} \right) \quad \text{when } W_c > 0 \quad (2)$$

The output  $W_c$  is a negligible positive signal (since the ratio of  $R_3$  to  $R_1$  is very small) and is not effective in regulating fuel flow. The diode does not conduct when the controller output  $W_c$  becomes negative, which occurs when an overtemperature condition causes the amplified temperature error signal to become positive (fig. 6). Equation (3) shows that the output signal with the diode open is that of proportional-plus-integral control action:

$$W_c = - \left( \frac{R_2}{R_1} + \frac{1}{R_1 C_2 s} \right) \frac{K_c T_e}{P_1} = - \left( K_a + \frac{1}{\tau_1 s} \right) \frac{K_c T_e}{P_1} \quad \text{when } W_c < 0 \quad (3)$$

The controller output can now regulate fuel flow and does so with a proportional-plus-integral control action. Fuel-flow regulation continues until  $W_c$  is zero and the diode conducts. The controller diode switching operates in the same manner for integral and proportional control systems.

### Engine Characteristics

The steady-state variation of tailpipe temperature with engine speed and fuel flow is shown in figure 7. These plots show a temperature reversal at 68.5-percent rated engine speed and 12.5-percent rated fuel flow. This results in a negative tailpipe-temperature to fuel-flow gain  $K_{TW}$  below 68.5-percent rated speed, as shown in figure 8. The engine gain is positive above 68.5-percent rated speed, reaching a maximum of 0.594 (percent rated temperature/percent fuel flow) at 86-percent rated speed.

The transient response of tailpipe temperature to fuel flow is of a lead-lag-plus-dead-time nature. The lead time constant  $\sigma_e$  and the lag time constant  $\tau_e$  decrease with engine speed as shown in figure 9. At 70-percent rated speed the lead time constant is  $2\frac{1}{2}$  times as large as the lag time constant. This ratio diminishes with engine speed, reaching unity at 100-percent speed where the engine lead equals the lag.

A tailpipe-temperature to fuel-flow dead time of approximately 55 milliseconds was observed for all engine speeds, as shown in figure 10. This dead time produces a 180° phase lag at 9 cycles per second. Figure 11 is a plot of the calculated forward-loop phase shift response with frequency, which includes the fuel system, engine dynamics, and the temperature-measuring circuit. A comparison of the total forward-loop phase shift with that of the tailpipe-temperature to fuel-flow dead time alone indicates that the forward-loop phase shift is primarily that of dead time.

### Control-Loop Characteristics

The control loop can be separated into two sections: (1) the forward path, which includes the fuel system, engine, and temperature instrumentation, and (2) the feedback path, which consists of the control components (fig. 12).

The transfer function of the forward path  $G(s)$  is composed of the cascaded fuel valve, engine, and temperature instrumentation transfer functions, as shown in the following equation:

$$G(s) = \frac{T_m s}{W_1 s - W_c s} = \frac{K_w K_{TW} K_m (1 + \sigma_e s)(1 + \sigma_c s)e^{-as}}{(1 + \tau_e s)(1 + \tau_c s)(1 + \tau_t s)} \quad (4)$$

Since the engine time constants and thermocouple lag change with engine speed, the forward-path frequency response varies with engine speed as shown in the calculated straight-line approximation of figure 13. The variation of thermocouple lag with engine speed has a cancelling effect on the amplitude spread resulting from the lower-frequency engine dynamics. It can be seen in figure 13 that the variation of amplitude ratio with engine speed is small beyond 0.6 cycle per second.

The transfer function of the feedback path  $H(s)$  consists of the transfer functions of the control amplifier and the controller (fig. 12). The controller response depends on the position of the diode switch. With the diode switch in the closed position ( $W_c > 0$ ), the transfer function is approximately zero. For control corrective action, the diode switch is open ( $W_c < 0$ ), and the transfer function is that of the particular controller action used. The transfer function with proportional-plus-integral control action is given in equation (5):

$$H(s) = \frac{W_c s}{T_s s - T_m s} = K_p + \frac{K_v}{s} \quad (5)$$

The transfer functions for proportional and integral control individually are  $K_p$  and  $K_v/s$ , respectively.

The loop gain  $G_L$  of the system at zero frequency is obtained from the frequency invariant components of the open-loop transfer function. Therefore, the loop gain with proportional control is  $K_w K_{TW} K_m K_p$ . Since the zero-frequency gain of the loop with integrating action is theoretically infinite, the loop gain is obtained from the loop velocity constant  $G_v$ , which is the product of the control velocity constant  $K_v$  and the forward-path gain  $K_w K_{TW} K_m$ .

#### PROCEDURE

The experimental program consisted of engine accelerations controlled by a temperature schedule. A ramp input to simulate a demand signal was used to obtain closed-loop transient response data. The transients were initiated from 62.5-percent rated engine speed where the steady-state operation is well below the scheduled temperature. A fixed ramp input of 2-second duration and a rate of 35-percent rated fuel flow per second were used for all transient tests.

The temperature schedule was set and maintained at 75-percent rated tailpipe temperature. This allowed a safe margin for overshoots, tracking errors, and steady-state errors for the various control gain settings used.

Data were obtained for both proportional and integral control with the gain varied from low settings to that sufficient to cause system instability. Proportional-plus-integral control data were obtained for independent variations of velocity constant and proportional gain.

The control systems were evaluated from the following criteria:

- (1) Loop gain and stability
- (2) Tracking error (velocity droop)
- (3) Steady-state error (positional droop)
- (4) First overshoot and large-slot opening overshoot

## DATA AND RESULTS

Typical transient data for proportional-plus-integral control action are shown in figure 14. The recorded traces are controller-output signal, fuel-valve position, engine speed, engine acceleration, and compensated tailpipe temperature.

From steady-state operation at 62.5-percent rated speed, a 2-second fuel ramp is applied to accelerate the engine at time labeled zero. The fuel-valve position  $W_f$  increases as a ramp until the measured temperature  $T_m$  exceeds the set temperature  $T_s$  as shown in figure 14 at 0.6 second. This activates the controller-output signal  $W_c$ , which reduces the fuel-valve position accordingly. At the termination of the 2-second ramp,  $W_c$  reverses to maintain the set temperature schedule.

A fuel-flow disturbance caused when the large-slot manifold fills and opens occurs during the time interval of 2.5 to 3.4 seconds in figure 14. At 2.5 seconds, the large-slot manifold begins to fill, reducing the effective fuel flow to the combustor. The controller output increases fuel flow to maintain the temperature schedule as shown by the fuel-valve-position increase during this interval. At 3.4 seconds the large slot opens and the effective fuel flow is too large, thereby causing a temperature overshoot at 3.6 seconds. This disturbance (large-slot overshoot) calls for corrective action by the controller. Although the fuel-system manifold filling characteristic is undesirable for maintaining a temperature schedule, the effectiveness of the controller to correct for a disturbance may be evaluated.

The ability of the controller to follow the temperature schedule is evaluated by three basic criteria: overshoot, velocity error, and positional error.

Two temperature overshoots are encountered, as shown in figure 14. The first overshoot occurs when the ramp fuel input accelerates the engine beyond the scheduled temperature, which activates the control system. A second overshoot takes place when the large-slot manifold opens to supply fuel to the engine.

Velocity or tracking errors of the system are of two forms, a positive error droop A and a negative error droop B. Droop A occurs when the controller signal is reducing fuel flow, such as during the period the fuel ramp input is in effect and the control is activated. A negative temperature error, droop B, occurs when the controller signal is increasing fuel flow to maintain the temperature schedule. Such a period is in evidence after the ramp fuel input is terminated until the

large slot opens. This droop is further divided into portions before and after the large-slot manifold starts filling its lines, labelled droops B and B<sub>L</sub>, respectively.

In trying to maintain set values at the end of a transient, steady-state or positional errors occur. No steady-state errors were involved with the integrating action of the feedback control used for figure 14.

#### Closed-Loop Control Data

Proportional control. - Proportional control data are presented in figure 15 for increasing values of control gain. The engine response to a low-gain proportional control ( $K_p = 3.25$ ) is presented in figure 15(a). The control output signal  $W_c$  shows that only a small correcting action takes place. This allows the fuel valve to follow the ramp input closely. Hence, these data are very similar to those of an uncontrolled system. The low proportional gain results in a system of poor regulation with a large-slot overshoot of 630° F and a steady-state error of 300° F.

Increasing the control gain to 13.0, as shown in figure 15(b), gives better control regulation. The large-slot overshoot temperature is reduced to 450° F with a steady-state error of 230° F. A slight amplification of temperature noise is evident on the fuel-valve-position trace.

The system is unstable, with small-amplitude oscillations for a proportional control gain of 39.0, as shown in figure 15(c). Although the increased proportional gain reduced large-slot overshoot to 290° F and steady-state error to 160° F, they remain of larger magnitude than can be tolerated for turbojet control. Amplification of noise has increased, particularly that of 60 cycles per second, resulting in large fuel-valve oscillations. Filtering of these objectionable frequencies is necessary for safe, smooth operation.

An unstable system with large oscillations results when control gain is increased to 45.5, as shown in figure 15(d). The unstable oscillation at the end of the transient has an amplitude of 335° F, with a frequency of 6.7 cycles per second. Large-slot overshoot is 255° F, with a steady-state error of 135° F.

As a result of these large steady-state errors, the proportional controller is undesirable. A plot of experimental and analytical steady-state error is shown for various loop gains in figure 16. (See appendix B for the analysis of steady-state-error derivation.) At a loop gain of unity, the steady-state error is about half that at zero loop gain. Any further increase in loop gain caused the system to become unstable.

Loop gain was restricted to approximately unity mainly by the large engine dead-time phase shift. At the unstable frequency of 6.7 cycles per second, the dead-time phase shift was  $130^\circ$ .

Integral control. - Transient data with integral control action are presented for increasing velocity constant in figure 17. The velocity constant  $K_v$  is increased from a low value of 130 in figure 17(a) to twice the gain (260) in figure 17(b). The use of integral control eliminates the final steady-state error. Doubling the velocity constant as shown in figures 17(a) and (b) had little effect on large-slot overshoot, a peak temperature of  $860^\circ$  F occurring in both cases. Velocity errors were reduced an average of 50 percent. The velocity tracking errors are relatively small compared with the large-slot overshoot error, that is, a maximum velocity error of  $55^\circ$  F compared with an overshoot error of  $240^\circ$  F.

Increasing the velocity constant to 520 results in an unstable system (fig. 17(c)). The instability that occurs when the control is engaged at low engine speed is of a low magnitude and becomes dampened during the filling of the large-slot manifold. The unstable amplitude is larger at higher engine speeds as a result of the larger engine gain, as shown previously in figure 8. The frequency of the unstable oscillations varied from 3 cycles per second at low engine speed to 2.85 cycles per second at the final engine speed.

Integral control action is more advantageous than proportional control, as it eliminated steady-state error and reduced tracking errors. The control loop becomes unstable at a frequency of 2.85 cycles per second with integral control action, compared with 6.7 cycles per second with proportional control action. An addition of proportional action to the integral control loop should provide increased stability.

Proportional-plus-integral. - A combination of increasing proportional gain to integral control is presented in figure 18. This set of data has a fixed velocity constant of 130, with proportional gain  $K_p$  varying from 3.25 to 45.5. The effect of increasing proportional gain in the control loop lowered large-slot peak overshoot from  $820^\circ$  F at  $K_p$  of 3.25 to  $715^\circ$  F at  $K_p$  of 45.5. This compares with a minimum overshoot of  $820^\circ$  F for integral action and  $875^\circ$  F with proportional action. The unstable frequency at the end of the transient of figure 18(d) is 6.0 cycles per second, which lies between that obtained for proportional and integral control individually.

#### Evaluation of Control Criteria

Steady-state error. - Steady-state positional errors occur with proportional control action only and decrease with increasing control

gain. At the maximum gain allowable for system stability, the steady-state error is too large to be suitable for turbojet-engine control.

Tracking error. - For integral and proportional-plus-integral control, both positive and negative tracking errors were observed. These temperature errors are of a constant nature and result from a constant rate of change of required controller output. A positive error that occurs when the control reduces fuel flow is called velocity error A. Calculation of this error, which is the same for both integral and proportional-plus-integral control, is presented in appendix B and is shown in equation (6):

$$T_{e,A} = \frac{K_I \sigma_e C_W - C_T}{1 + K_I \sigma_e K_V} \quad (6)$$

A plot of velocity error against control velocity constant (fig. 19) indicates that the calculated velocity droop A follows the experimental results closely. Increasing velocity constant reduces the tracking error.

A negative tracking error that results when the controller increases fuel flow is called velocity droop B. Such an error occurs after the fuel-ramp input is terminated, and calculations of this error are presented in appendix B. Equation (7) shows that the calculated droop B is similar to droop A of equation (6) without the positive term in the numerator:

$$T_{e,B} = \frac{-C_T}{1 + K_I \sigma_e K_V} \quad (7)$$

The value of droop B, which diminishes with increased velocity constant, is also shown in figure 19.

A third tracking error occurs when the filling of the large-slot subtracts from the effective fuel flow to the engine. This error is larger than droop B, and insufficient information was available for its calculation. The experimental data for large-slot droop are shown in figure 19.

Overshoot error. - Temperature overshoot errors from large input signals were found to be larger than tracking errors. Therefore, the temperature overshoots resulting from ramp fuel input and the large-slot openings are more critical in the evaluation of a safe control for surge prevention.

The fuel-ramp-induced temperature overshoot is plotted with proportional gain for several values of velocity constant in figure 20(a).

Small variations of temperature overshoot occur when proportional gain is varied, with a minimum value at a proportional control gain of 26. The temperature overshoot variation with velocity constant (fig. 20(b)) indicates a minimum value at a control velocity constant of 260. Therefore, the proportional-plus-integral control setting for minimizing the fuel-ramp-induced temperature overshoot is  $K_p$  of 26 and  $K_v$  of 260.

The large-slot temperature overshoot occurs at a higher engine speed and is of a larger magnitude. Plots of large-slot overshoot with increasing proportional and velocity constant control gains are shown in figures 21(a) and (b), respectively. A reduction in large-slot temperature overshoot with increasing control gain for both proportional and integral control is shown by the data.

Selecting the optimum control gain for minimizing the fuel-ramp temperature overshoot ( $K_p$  of 26 and  $K_v$  of 260) produces a large-slot overshoot error of  $155^\circ\text{F}$ . The large-slot overshoot error is the largest error involved in tracking the temperature schedule. Therefore, selecting a margin between scheduled temperature and surge-line temperature will depend primarily on this error.

Stability limit. - Stability problems develop in an attempt to improve the transient response by increasing the control gain. The transient data previously shown in figure 15 are typical of the oscillatory growth with increases of control gain. A stability-limit plot for variations of both proportional and velocity constant control gains is shown in figure 22. Proportional control data lie on the ordinate, whereas integral control data fall on the abscissa. Lines of constant proportional-plus-integral relation radiate from the origin toward the unstable region. The stability limit calculated at 94-percent rated speed is between the experimental data of stable and unstable operation.

The calculated frequency for instability decreases from 6.5 cycles per second to 2.9 cycles per second as the control varies from proportional to integral operation. In general, the system becomes more unstable as either control gain is increased. An exception occurs from the reversal of the stability limit near the integral control axis (fig. 22). When operating at an unstable velocity constant of 500, the system becomes stable with the addition of proportional control gain from 8 to 21.

#### Application of Temperature Schedule Control

The turbojet engine used for the experimental investigation had an acceleration margin in the surge region that varied from 30 to 50 percent of rated temperature. Temperature errors that existed for the optimum proportional-plus-integral control action were less than 2-percent

rated temperature for the first overshoot and velocity errors, whereas the large-slot overshoot equalled 10-percent rated temperature. Elimination of the flow-divider dynamics would result in control schedule deviations within 2-percent rated temperature for an input of 35-percent rated fuel flow per second.

#### CONCLUDING REMARKS

The temperature-acceleration control design encompasses an adjustment for (1) engine dynamics and temperature-sensor variations with engine speed, (2) thermocouple compensation, (3) engine dead time, and (4) choice of controller action.

The tailpipe-thermocouple time-lag variations tend to cancel the engine lead-lag variation with engine speed. Steady-state engine gain variations result in large changes of loop gain with engine speed. This difficulty may be alleviated by a compensating gain schedule.

An accurate measurement of temperature is needed, particularly in the low-speed operating region where surge is the acceleration limit. Frequency response was extended by the use of a thermocouple compensator critically set in the low-speed region. This compensator setting produced an overcompensated or safer temperature measurement in the higher-speed region where temperature is the acceleration limit.

The tailpipe-temperature deviations from the set schedule during an acceleration were of three types: temperature overshoots, velocity errors, and steady-state errors.

The overshoot of controlled temperature is the largest temperature error encountered and is the primary factor in selecting a safe margin between scheduled and undesirable temperatures.

Velocity error was observed for integral and proportional-plus-integral control schemes. The velocity errors are of both positive and negative nature, depending on the control output correcting action. The velocity droop is predictable analytically, decreases with increasing velocity constant, and is small when compared with large-slot overshoot temperature error.

Steady-state positional errors occur with proportional control only and decrease with increasing loop gain. The steady-state error is analytically predictable but was too large to be suitable for a turbojet-engine control.

Stability limits are analytically predictable with close agreement to experimental data. The engine dead time is an appreciable factor towards control-loop instability, particularly with proportional-type control. The frequency at which the system becomes unstable is highest for proportional control and lowest with integral control. The addition of some proportional gain to a slightly unstable integral control system has a stabilizing influence.

The most favorable control system tested was that of proportional-plus-integral action, which had no steady-state error, minimum tracking and overshoot error, and a higher velocity-constant stability limit.

Lewis Flight Propulsion Laboratory  
National Advisory Committee for Aeronautics  
Cleveland, Ohio, April 5, 1956

## APPENDIX A

## SYMBOLS

The following symbols are used in this report:

a	dead time of tailpipe temperature to fuel flow, sec
C	capacitive component
$C_T$	set temperature constant
$C_W$	fuel input rate constant
$G_L$	loop gain at zero frequency
$G_V$	loop velocity constant
$K_a$	gain of controller amplifier, $R_2/R_1$
$K_c$	fixed gain of control amplifier, $K_c = R_6/R_4 = R_6/R_5$
$K_m$	gain of temperature sensor and compensator
$K_p$	proportional control gain, $\frac{K_c K_a}{P_1}$
$K_{TW}$	engine gain of tailpipe temperature to fuel flow
$K_v$	control velocity constant
$K_w$	gain of fuel flow to fuel system input voltage
$K_1$	gain from fuel servomotor input to compensator output, $K_1 = K_w K_{TW} K_m$
N	engine speed, percent rated
P	potentiometer setting
R	resistive component
s	operational form of Laplace operator
T	tailpipe temperature, °F
$T_e$	temperature error between set temperature and measured temperature, °F

$T_m$	measured tailpipe temperature, °F
$T_s$	scheduled temperature, °F
$t$	time, sec
$W_c$	controller output signal
$W_f$	fuel-valve position
$W_i$	input demand signal
$\sigma_c$	thermocouple compensator lead time constant, sec
$\sigma_e$	engine lead time constant, sec
$\tau_c$	thermocouple-compensator lag time constant, sec
$\tau_e$	engine lag time constant, sec
$\tau_i$	control integrator time constant, sec
$\tau_t$	thermocouple lag time constant, sec
$\omega$	frequency, cps

**Subscripts:**

A	velocity error occurring when control reduces fuel flow
B	velocity error occurring when control increases fuel flow
1,2,3...	designation of resistor, potentiometer, or capacitance from fig. 6

**Transfer functions:**

$C(s)$	controller output to temperature error
$E(s)$	engine tailpipe temperature to fuel flow
$G(s)$	forward path (measured temperature to fuel system input)
$H(s)$	feedback path (controller output to control amplifier input)
$M(s)$	thermocouple-compensator output to tailpipe temperature
$W(s)$	fuel flow to fuel-system input

## APPENDIX B

## DERIVATION OF EQUATIONS

## Velocity Error

The derivation of velocity droop is obtained from the basic closed-loop system with its associated transfer functions as shown in figure 12. The forward transfer function  $G(s)$  consists of the fuel system, the turbojet engine, and the temperature-measuring components.

Experimental velocity errors occurred from 70 to 75 percent of rated engine speed. In this region, the engine dynamics have a small steady-state gain (fig. 8) and a large engine lead time constant (fig. 9). Because the frequency variant term is large compared with the frequency invariant term, the engine lead  $(1 + \sigma_e s)$  can be assumed to be a pure derivative  $\sigma_e s$ . The forward transfer function with the engine derivative assumption is as follows:

$$G(s) = \frac{K_1 \sigma_e s (1 + \sigma_c s) e^{-as}}{(1 + \tau_e s)(1 + \tau_t s)(1 + \tau_c s)} \quad (B1)$$

where  $K_1 = K_w K_{TW} K_m$ .

The feedback path consists of the temperature schedule-maintaining control transfer function  $H(s)$ . For proportional control action, the experimental temperature error never reached a constant velocity error and therefore is not derived. Integral and proportional-plus-integral control actions were investigated and are presented in equations (B2) and (B3), respectively:

$$H(s) = \frac{K_c}{P_1 \tau_1 s} = \frac{K_v}{s} \quad (\text{Integral action}) \quad (B2)$$

$$H(s) = \frac{K_c K_a}{P_1} + \frac{K_c}{P_1 \tau_1 s} = K_p + \frac{K_v}{s} \quad (\text{Proportional plus integral action}) \quad (B3)$$

The temperature error  $T_e$  with respect to fuel-flow input  $W_1$  and scheduled temperature  $T_s$  is derived in equation (B4):

$$T_e(s) = \frac{G(s)}{[1 + G(s)H(s)]} W_1(s) - \frac{1}{[1 + G(s)H(s)]} T_s(s) \quad (B4)$$

Droop A. - The temperature tracking error, droop A, resulted from a ramp input of fuel flow with the scheduled temperature fixed at its set value. These forcing functions in their operational form are

$$W_1(s) = \frac{C_W}{s^2}$$

and

$$T_S(s) = \frac{C_T}{s}$$

which, applied to the general temperature-error equation (B4), produce the temperature-error response:

$$\begin{aligned} T_{e,A}(s) &= \frac{G(s)}{[1 + G(s)H(s)]} \left( \frac{C_W}{s^2} \right) - \frac{1}{[1 + G(s)H(s)]} \left( \frac{C_T}{s} \right) \\ &= \frac{G(s)C_W - C_T s}{s^2 [1 + G(s)H(s)]} \end{aligned} \quad (B5)$$

When the values of  $G(s)$  and  $H(s)$  for proportional-plus-integral control are inserted, the tracking error takes the following form:

$$\begin{aligned} T_{e,A}(s) &= \frac{K_1 \sigma_e s (1 + \sigma_c s) C_W e^{-as}}{(1 + \tau_e s)(1 + \tau_t s)(1 + \tau_c s)} - \frac{s C_T}{s^2 \left[ 1 + \frac{K_1 \sigma_e s (1 + \sigma_c s) (s K_p + K_v) e^{-as}}{(1 + \tau_e s)(1 + \tau_t s)(1 + \tau_c s) s} \right]} \end{aligned} \quad (B6)$$

Applying the final value theorem from reference 5

$$\lim_{t \rightarrow \infty} f(t) = \lim_{s \rightarrow 0} sF(s)$$

results in a constant velocity error, droop A, as follows:

$$T_{e,A} = \frac{K_1 \sigma_e C_W - C_T}{1 + K_1 \sigma_e K_v} \quad (B7)$$

Since the proportional control term  $sK_p$  in equation (B6) approaches zero with the application of the final value theorem, the droop A equation (B7) is valid for both integral and proportional-plus-integral control action.

Droop B. - The derivation of droop B is obtained from equation (B4) after the termination of the ramp fuel input. Therefore, constant-value functions are applied to both  $W_1(s)$  and  $T_B(s)$ :

$$T_{e,B}(s) = \frac{G(s)}{[1 + G(s)H(s)]} \frac{C_W}{s} - \frac{1}{[1 + G(s)H(s)]} \frac{C_T}{s} \quad (B8)$$

Using proportional-plus-integral control action and applying the final value theorem give droop B:

$$T_{e,B} = \frac{0 - C_T}{1 + K_1 \sigma_e K_v} \quad (B9)$$

As indicated by equation (B9), the velocity error, droop B, is the same for both proportional-plus-integral and integral control.

#### Steady-State Error

The ability of a control parameter to seek its set value at the end of a transient is important to avoid unsafe operation. The equations derived in this section determine the steady-state errors for various control gains and control schemes.

From the block diagram in figure 12, the temperature error  $T_e$  with respect to fuel-flow input  $W_1$  and scheduled temperature  $T_B$  is as follows:

$$\begin{aligned} T_e(s) &= \left[ \frac{G(s)}{1 + G(s)H(s)} \right] W_1(s) - \left[ \frac{1}{1 + G(s)H(s)} \right] T_B(s) \\ &= \frac{G(s)W_1(s) - T_B(s)}{1 + G(s)H(s)} \end{aligned} \quad (B10)$$

Constant-value forcing functions are applied to  $W_1(s)$  and  $T_S(s)$  in order to obtain the temperature-error response with proportional control action:

$$T_e(s) = \frac{\left( \frac{K_1(1 + \sigma_e s)(1 + \sigma_c s)e^{-as}}{(1 + \tau_e s)(1 + \tau_c s)(1 + \tau_t s)} \right) \left( \frac{C_w}{s} \right) - \frac{C_T}{s}}{1 + \left( \frac{K_1(1 + \sigma_e s)(1 + \sigma_c s)e^{-as}}{(1 + \tau_e s)(1 + \tau_c s)(1 + \tau_t s)} \right) K_p} \quad (B11)$$

Applying the final value theorem to equation (B11) results in the steady-state temperature error:

$$T_e = \frac{K_1 C_w - C_T}{1 + K_1 K_p} \quad (B12)$$

Adding an integrator to a control system and applying the final value theorem result in a zero steady-state error.

#### REFERENCES

1. Stiglic, Paul M., Schmidt, Ross D., and Delio, Gene J.: Experimental Investigation of Acceleration Characteristics of a Turbojet Engine Including Regions of Surge and Stall for Control Applications. NACA RM E54H24, 1954.
2. Novik, David, Heppler, Herbert, and Stiglic, Paul M.: Experimental Investigation of a Surge Control on a Turbojet Engine. NACA RM E55H03, 1955.
3. Stiglic, Paul M., Heppler, Herbert J., and Novik, David: Experimental and Analytical Investigation of an Acceleration Regulating Control for a Turbojet Engine. NACA RM E56C07.
4. Otto, Edward W., Gold, Harold, and Hiller, Kirby W.: Design and Performance of Throttle-Type Fuel Controls for Engine Dynamics Studies. NACA TN 3445, 1955.
5. Chestnut, Harold, and Mayer, Robert W.: Servomechanisms and Regulating System Design. Vol. 1. John Wiley & Sons, Inc., 1951.

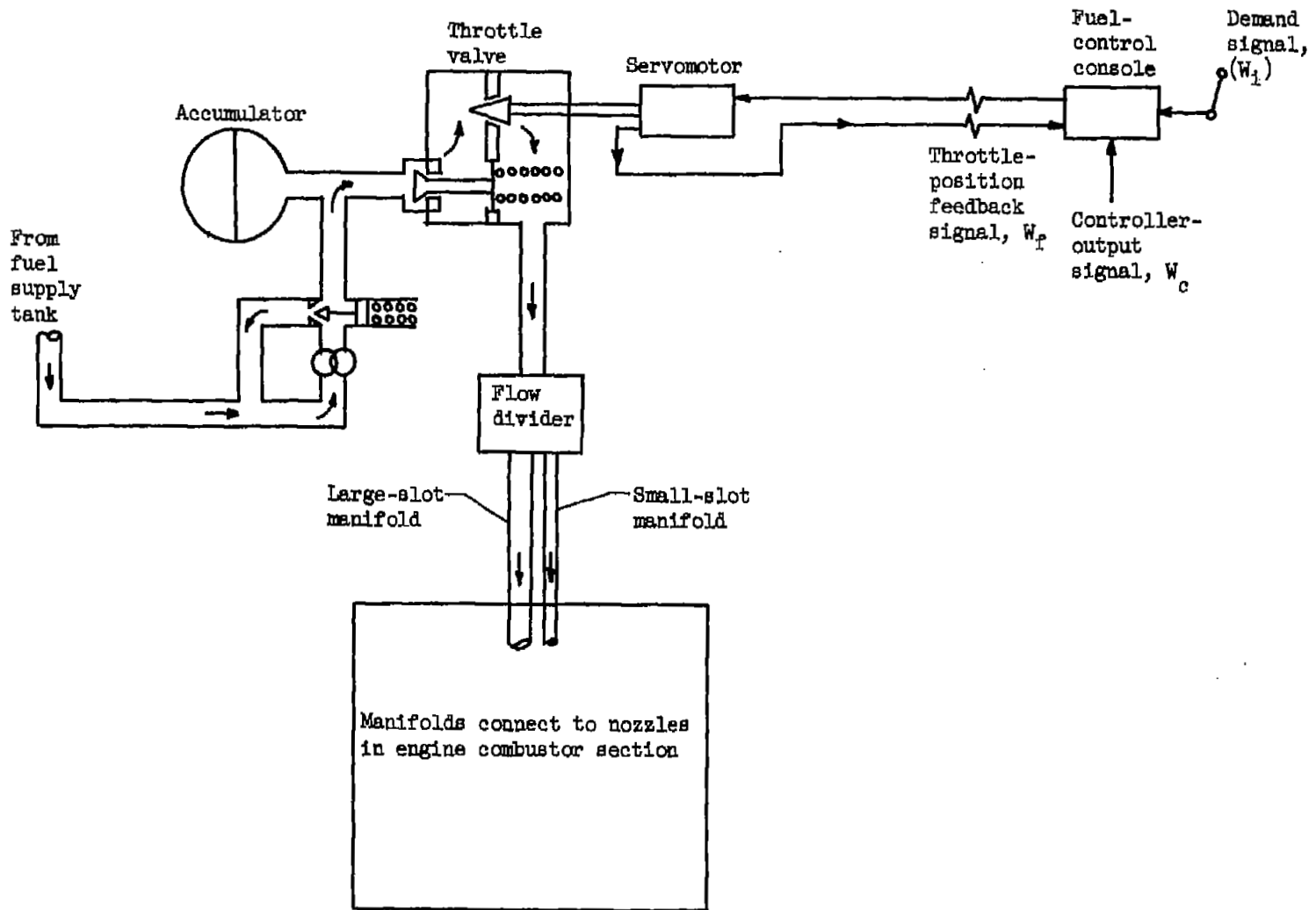


Figure 1. - Fuel system with reducing-type differential pressure regulator.

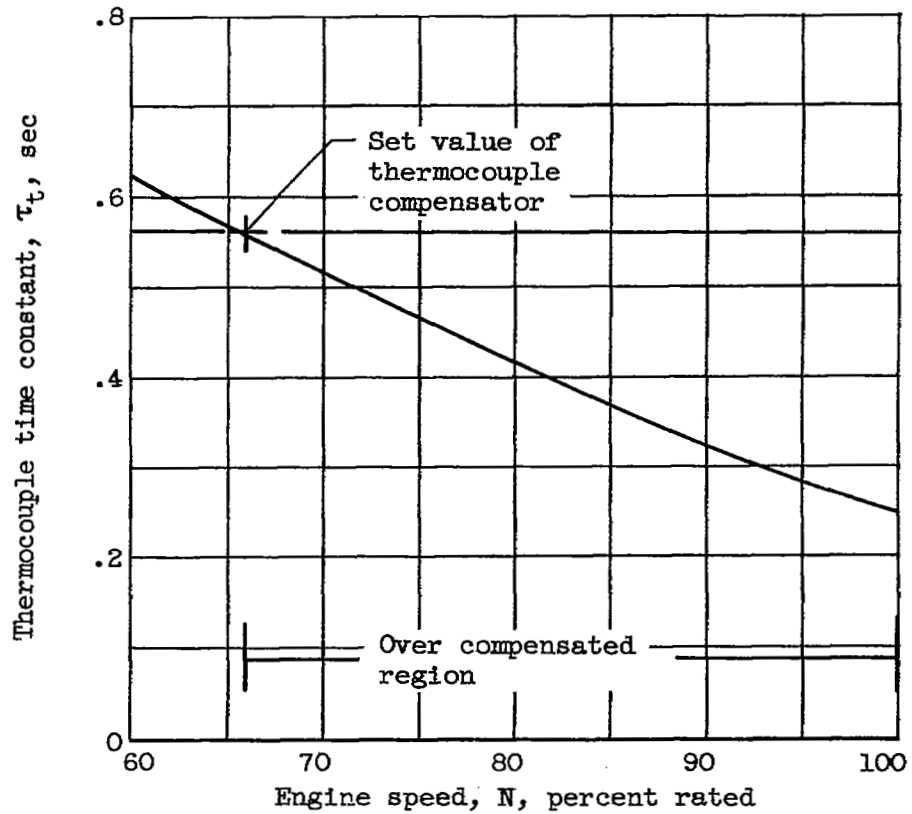


Figure 2. - Variation of thermocouple lag first-order approximation over operating range of engine.

3974

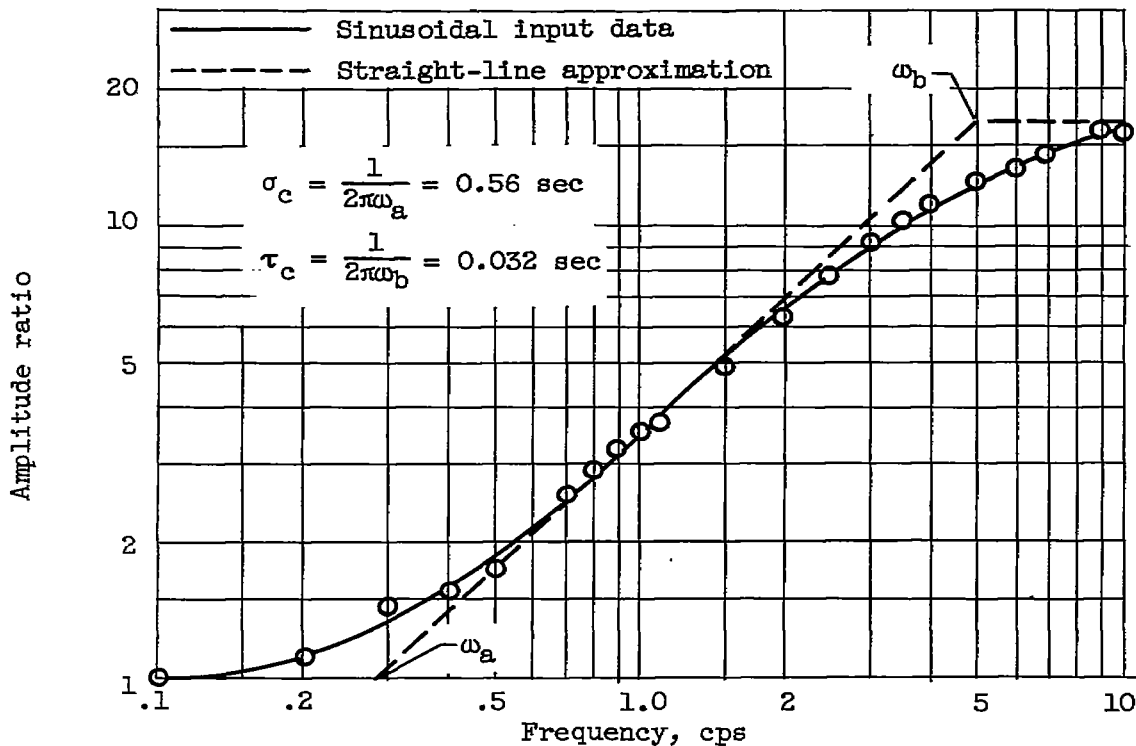


Figure 3. - Thermocouple compensator frequency response with lead time constant set for complete compensation at 66 per-cent rated engine speed.

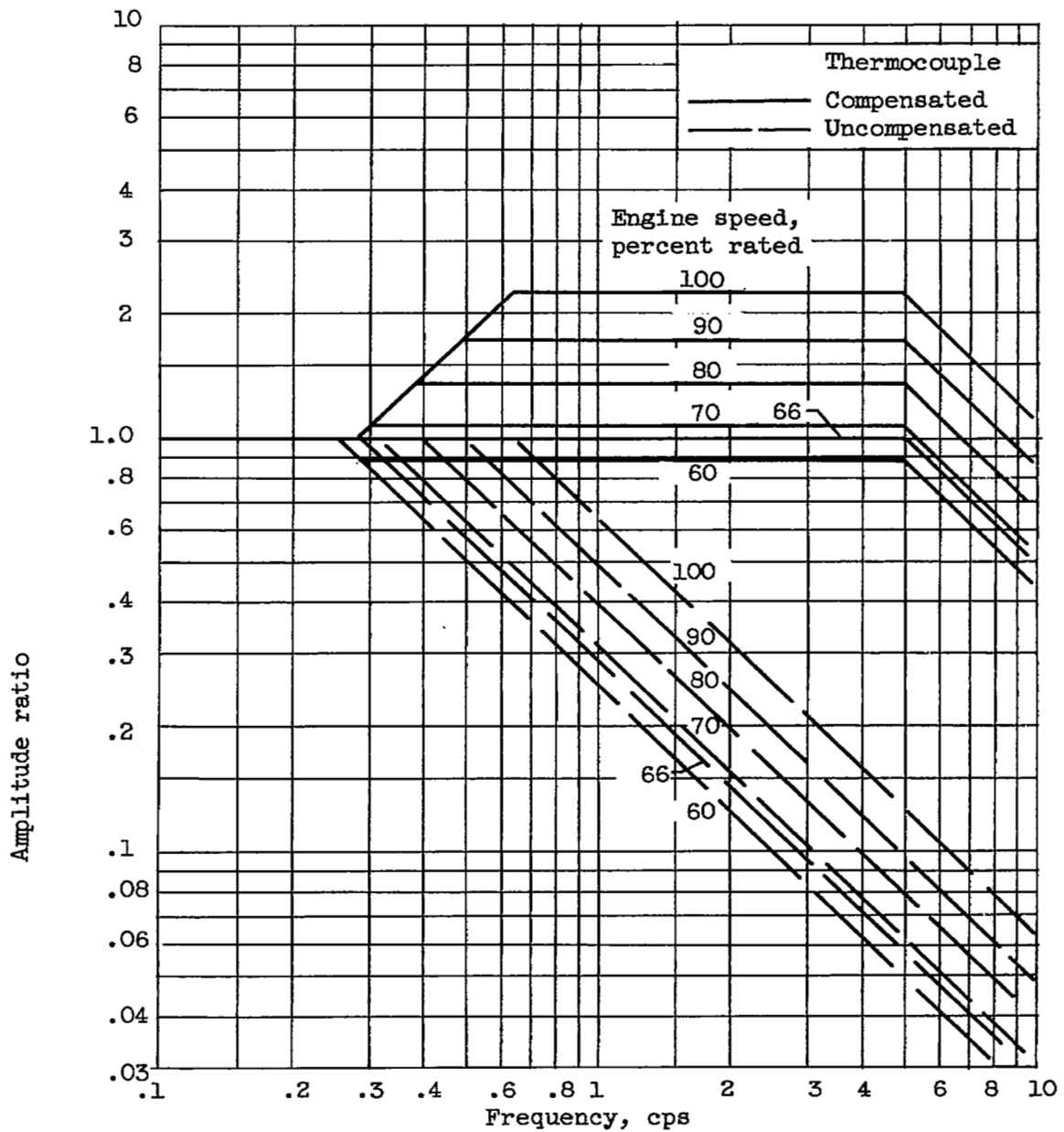


Figure 4. - Comparison of frequency response for compensated and uncompensated tailpipe thermocouple over operating speed range of engine. Compensation matched at 66 percent rated engine speed.

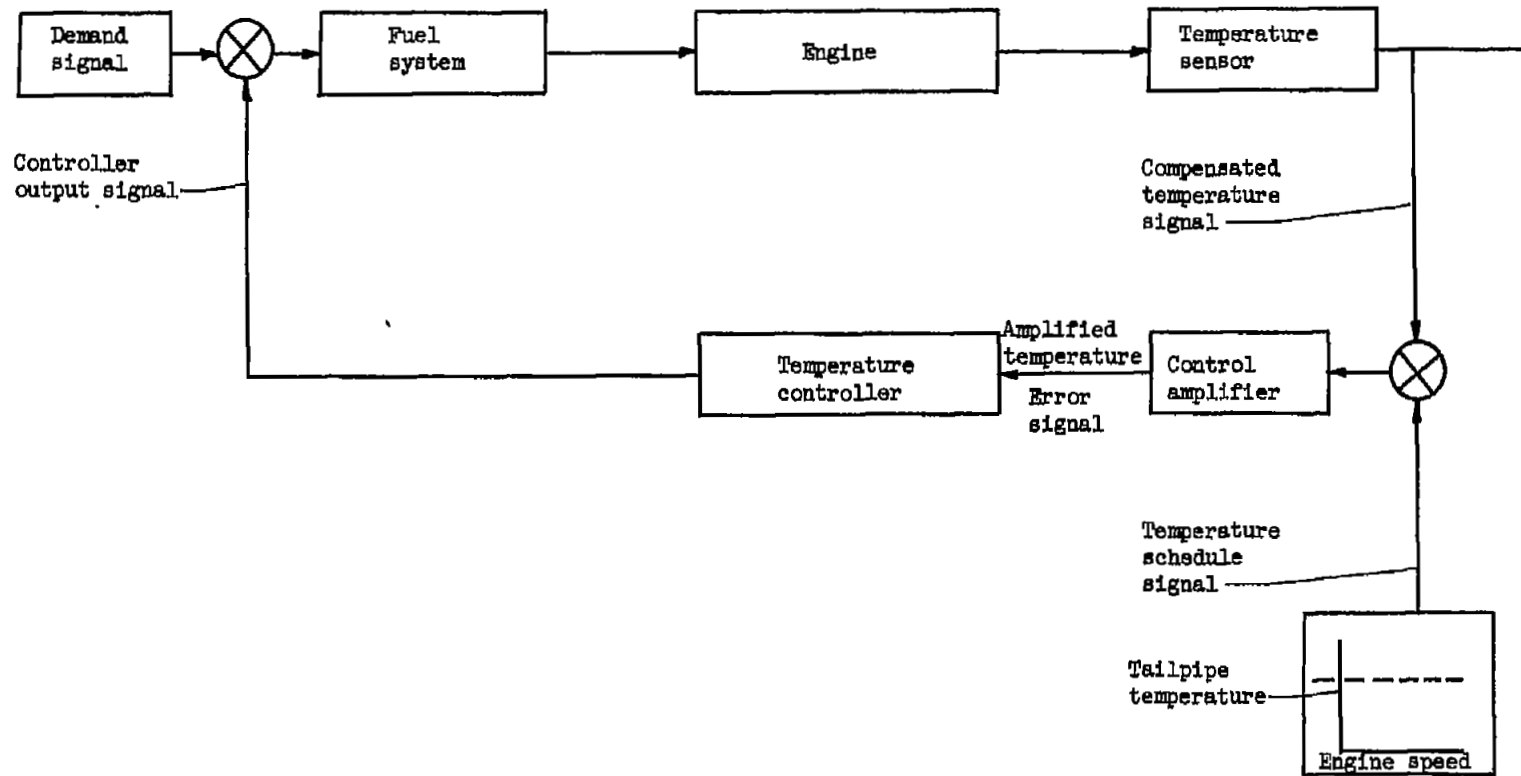
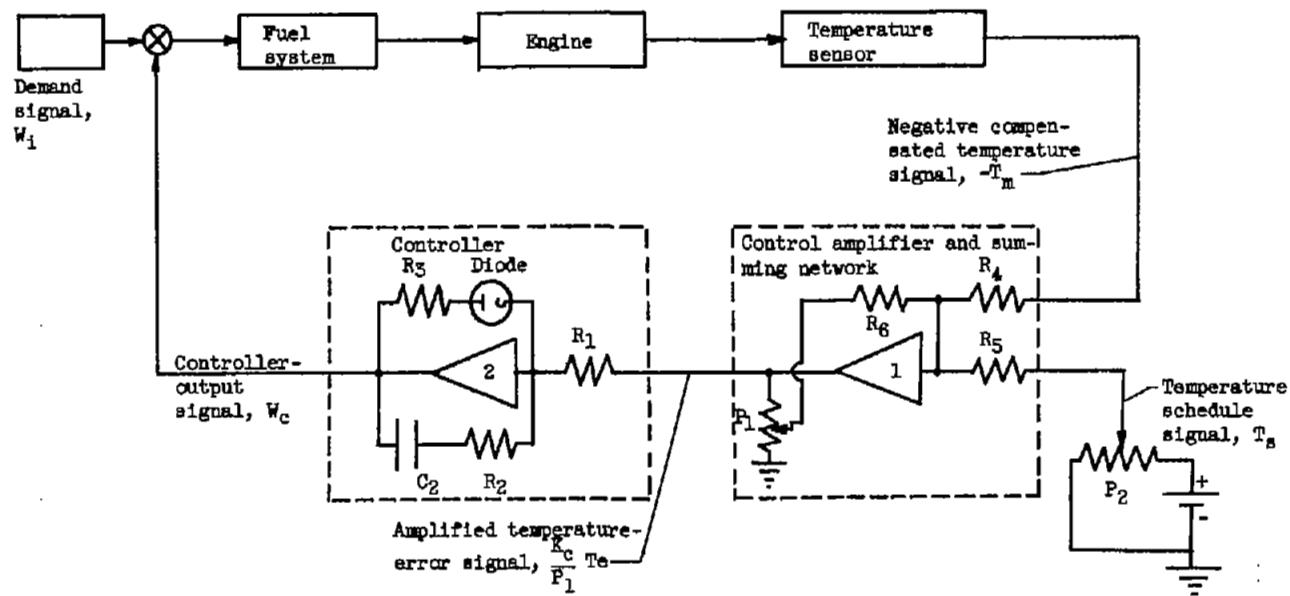


Figure 5. - Control loop for temperature-scheduling acceleration control.

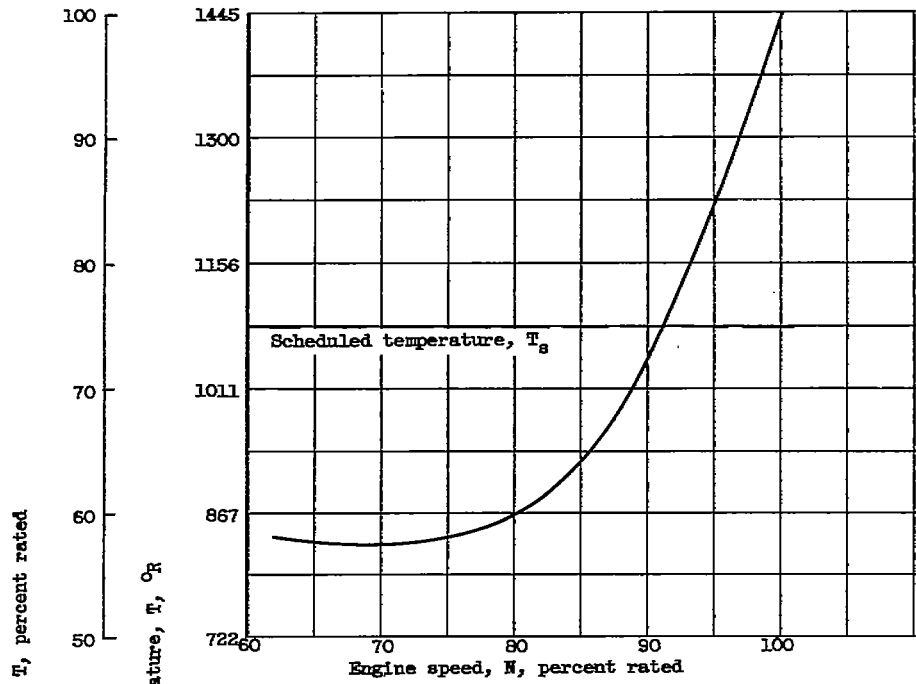


Controller transfer function ( $R_3 \ll R_1$ )		
	Diode switch position	
	$W_c > 0$ (Diode conducts)	$W_c < 0$ (Diode open)
Proportional configuration ( $R_2$ in) ( $C_2$ out)	$\frac{R_3 R_2}{R_1(R_3 + R_2)} = 0$	$\frac{R_2}{R_1} = K_a$
Integral configuration ( $R_2$ out) ( $C_2$ in)	$\frac{R_3}{R_1(1 + R_3 C_2 s)} = 0$	$\frac{1}{R_1 C_2 s} = \frac{1}{\tau_1 s}$
Proportional plus integral configuration ( $R_2$ in) ( $C_2$ in)	$\frac{R_3(1 + R_2 C_2 s)}{R_1(1 + R_2 C_2 s + R_3 C_2 s)} = 0$	$\frac{R_2}{R_1} + \frac{1}{R_1 C_2 s} = K_a + \frac{1}{\tau_1 s}$

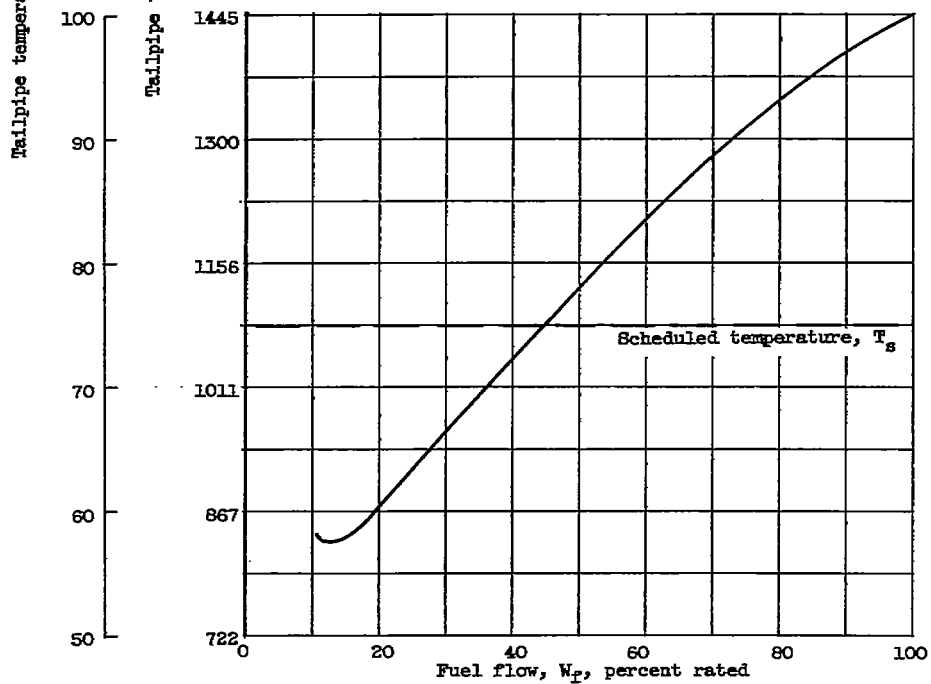
Figure 6. - Temperature-control circuit.

3974

CD-4 back



(a) Engine speed.



(b) Fuel flow.

Figure 7. - Variation of tailpipe temperature with two engine parameters.

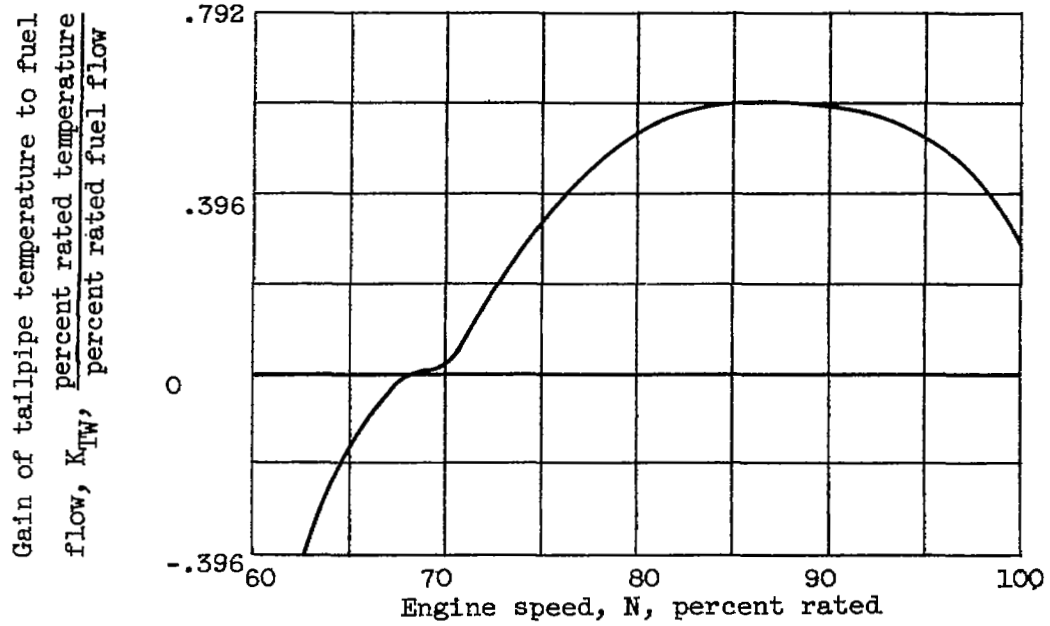


Figure 8. - Variation of engine gain with engine speed.

3974

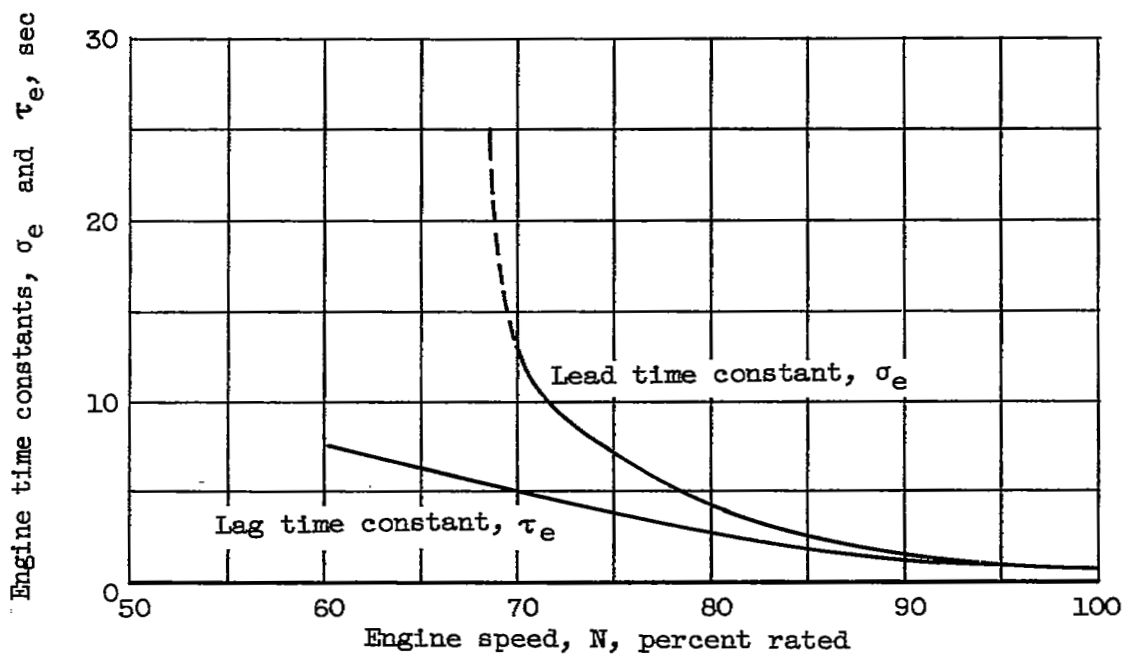


Figure 9. - Variation of engine time constants with engine speed.

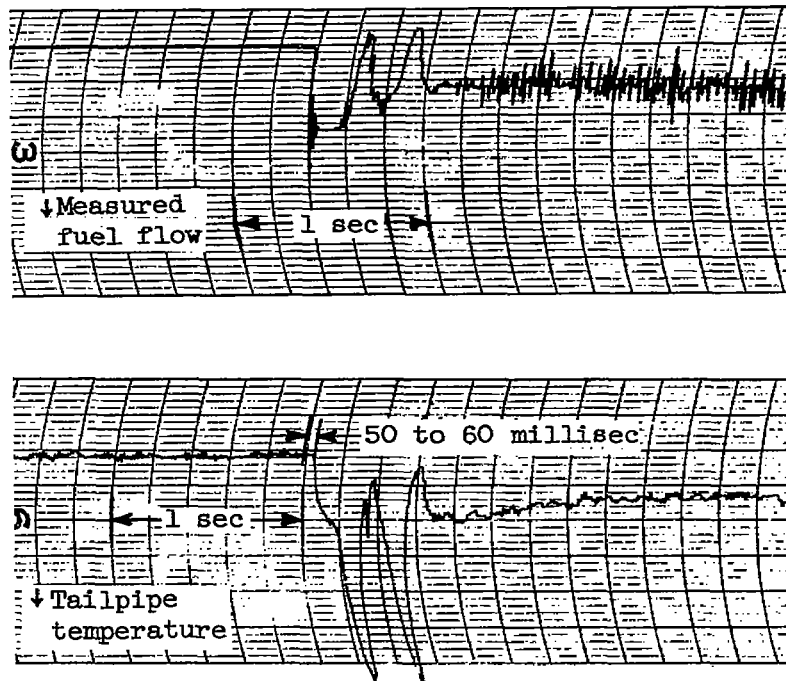


Figure 10. - Typical dead-time response of tailpipe temperature to fuel flow.

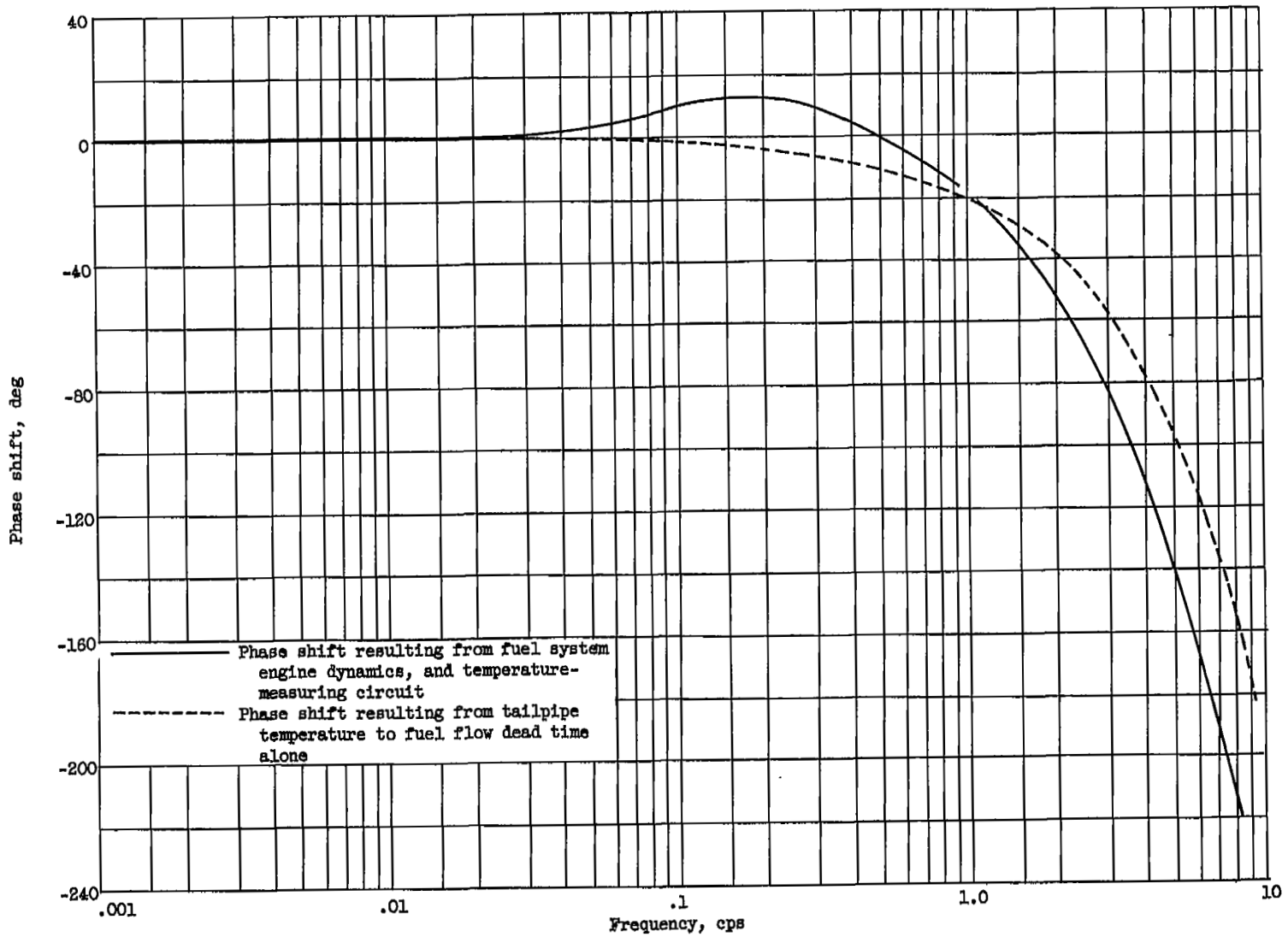


Figure 11. - Comparison of total calculated forward loop phase shift with that of tailpipe temperature to fuel flow dead time alone at 94 percent rated engine speed.

$$G(s) = W(s) E(s) M(s) = \frac{K_1 (1 + \sigma_e s)(1 + \sigma_c s) e^{-as}}{(1 + \tau_e s)(1 + \tau_c s)(1 + \tau_t s)} \quad (\text{where: } K_1 = K_w K_{TW} K_m)$$

$$= 0.0426 K_{TW} \left( \frac{\text{percent rated, } W_F}{\text{percent rated, } T} \right)$$

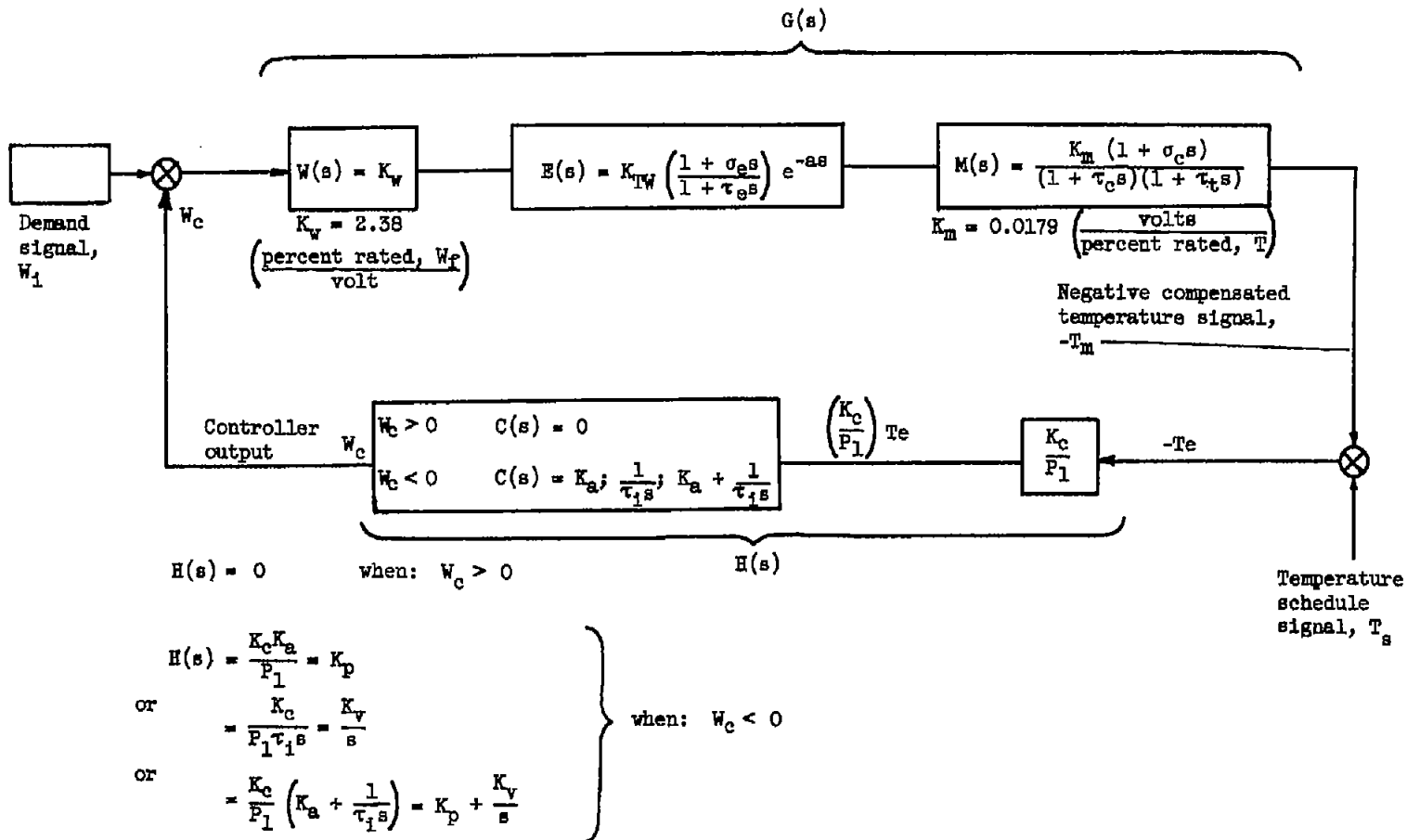


Figure 12. - Transfer functions of forward and controller paths from individual control-loop components.

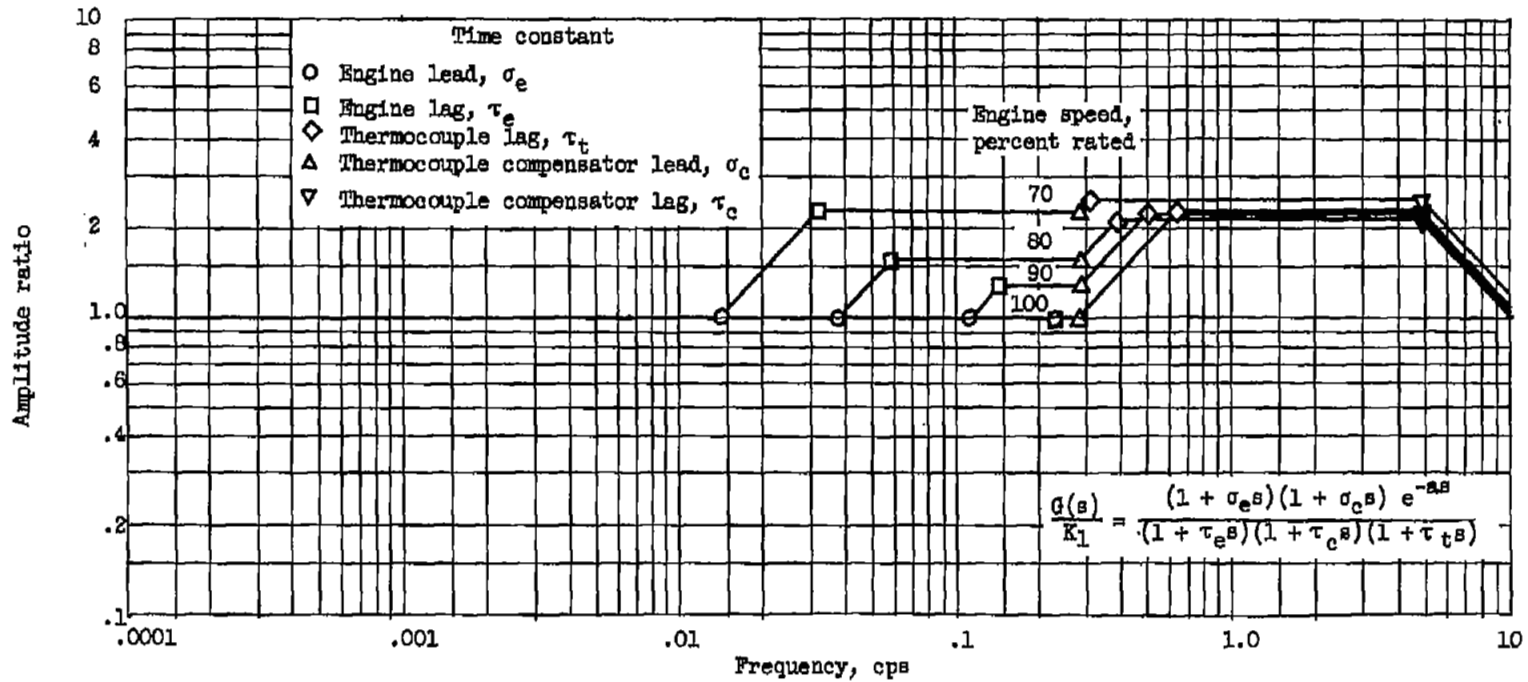


Figure 13. - Variation of calculated forward path frequency response with engine speed.

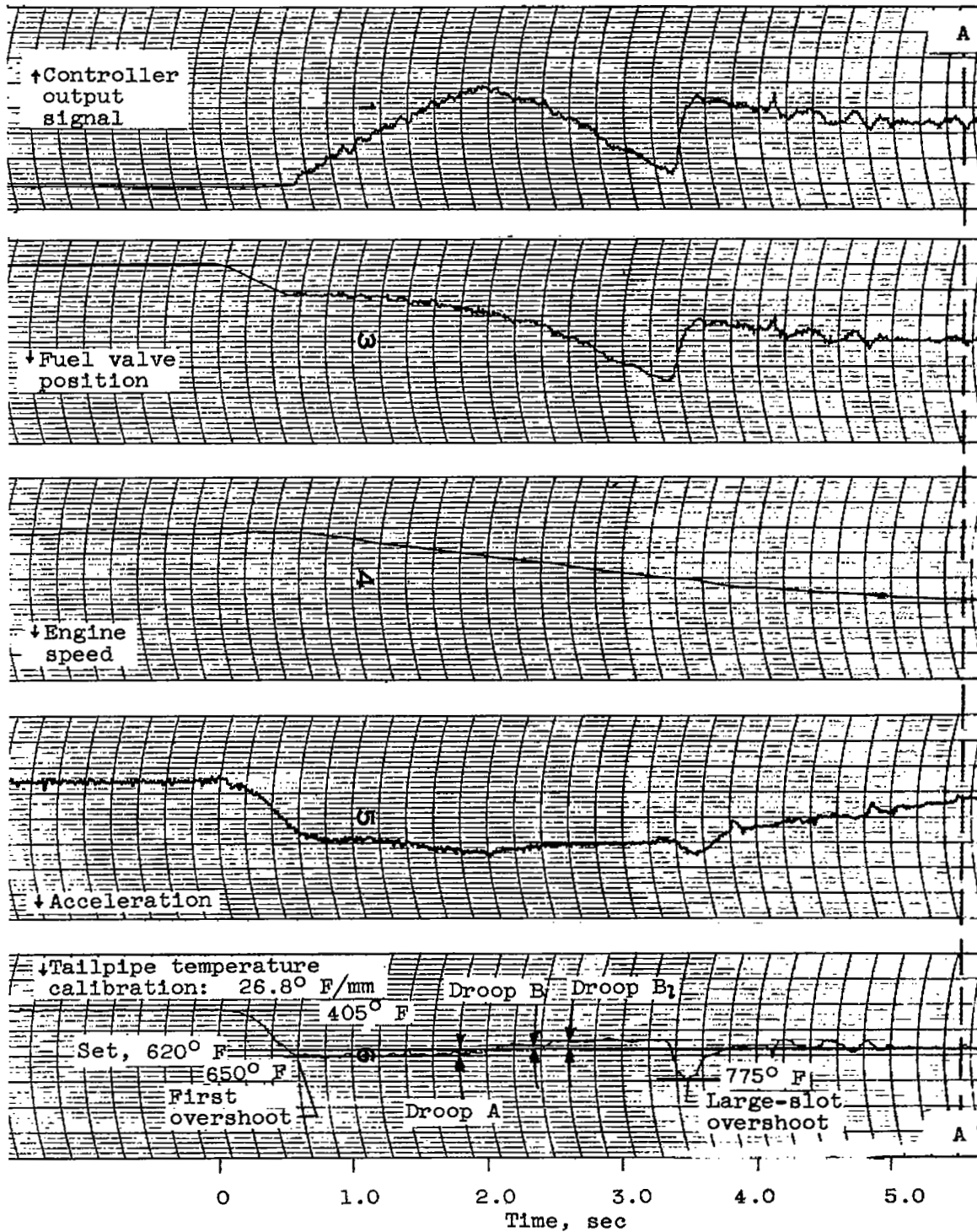
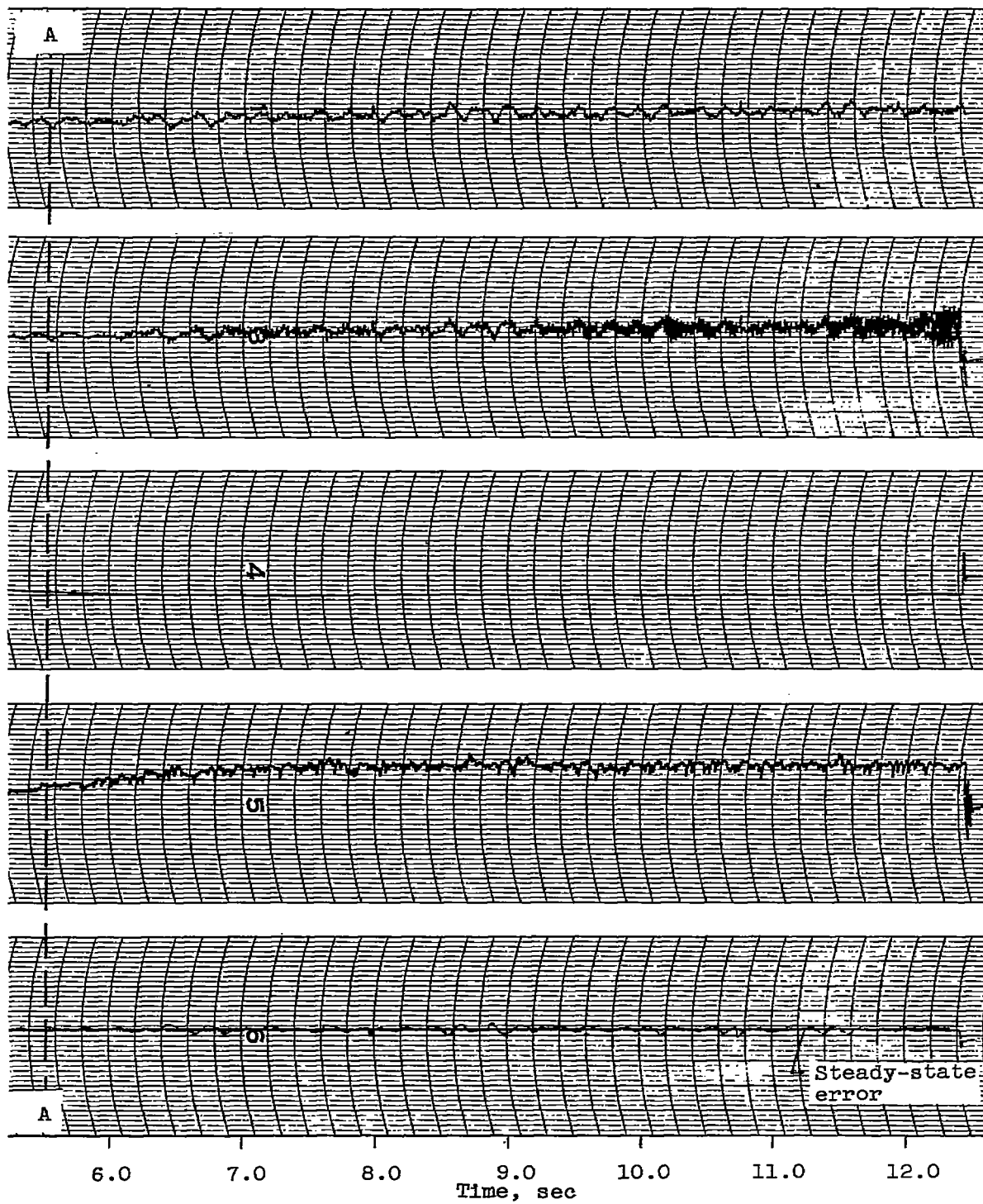
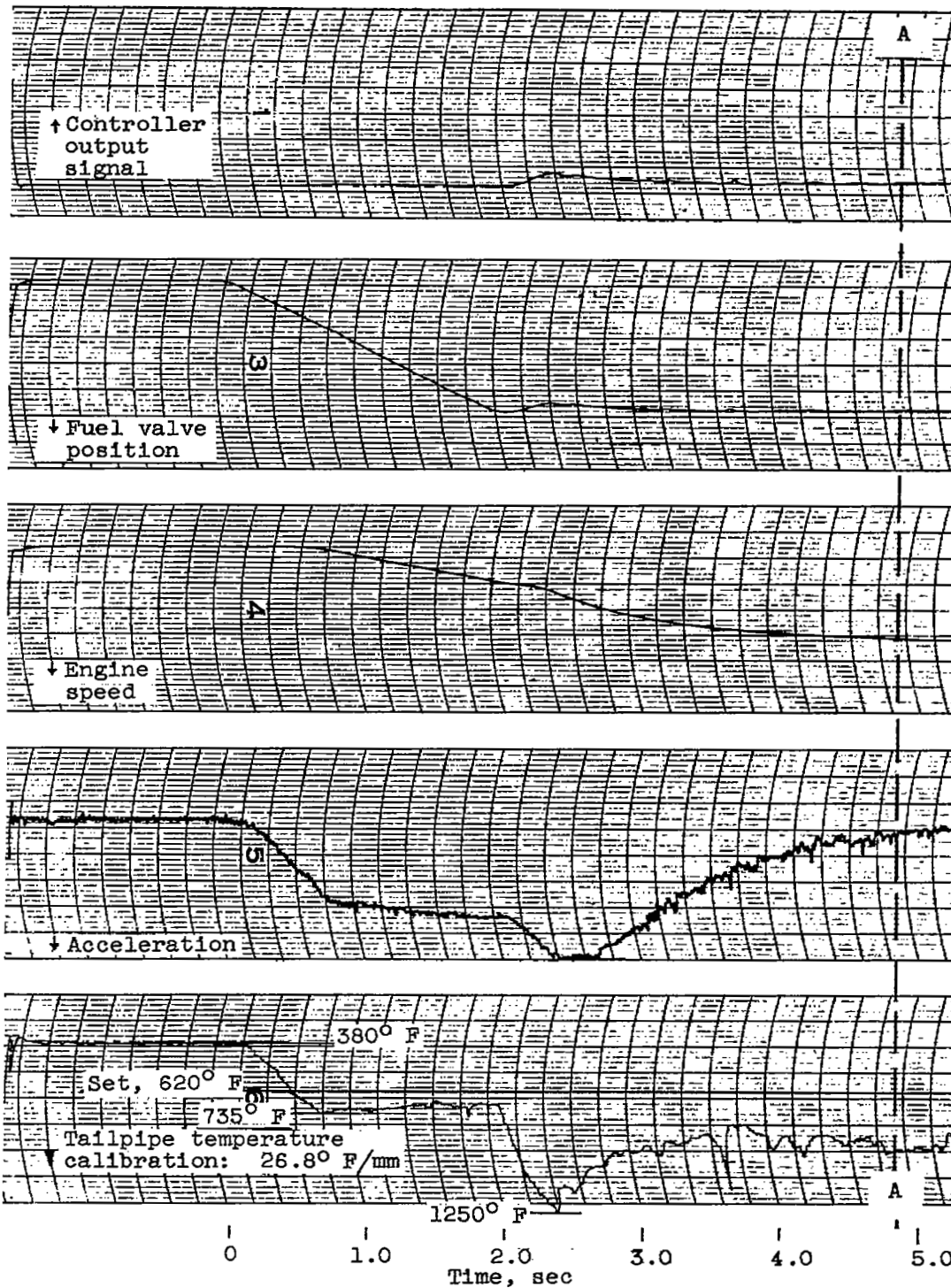


Figure 14. - Typical response of control to ramp fuel input for proportional-plus-integral control action. Ramp input, 2500 pounds per hour per second for 2 seconds.

3974

CD-5 back

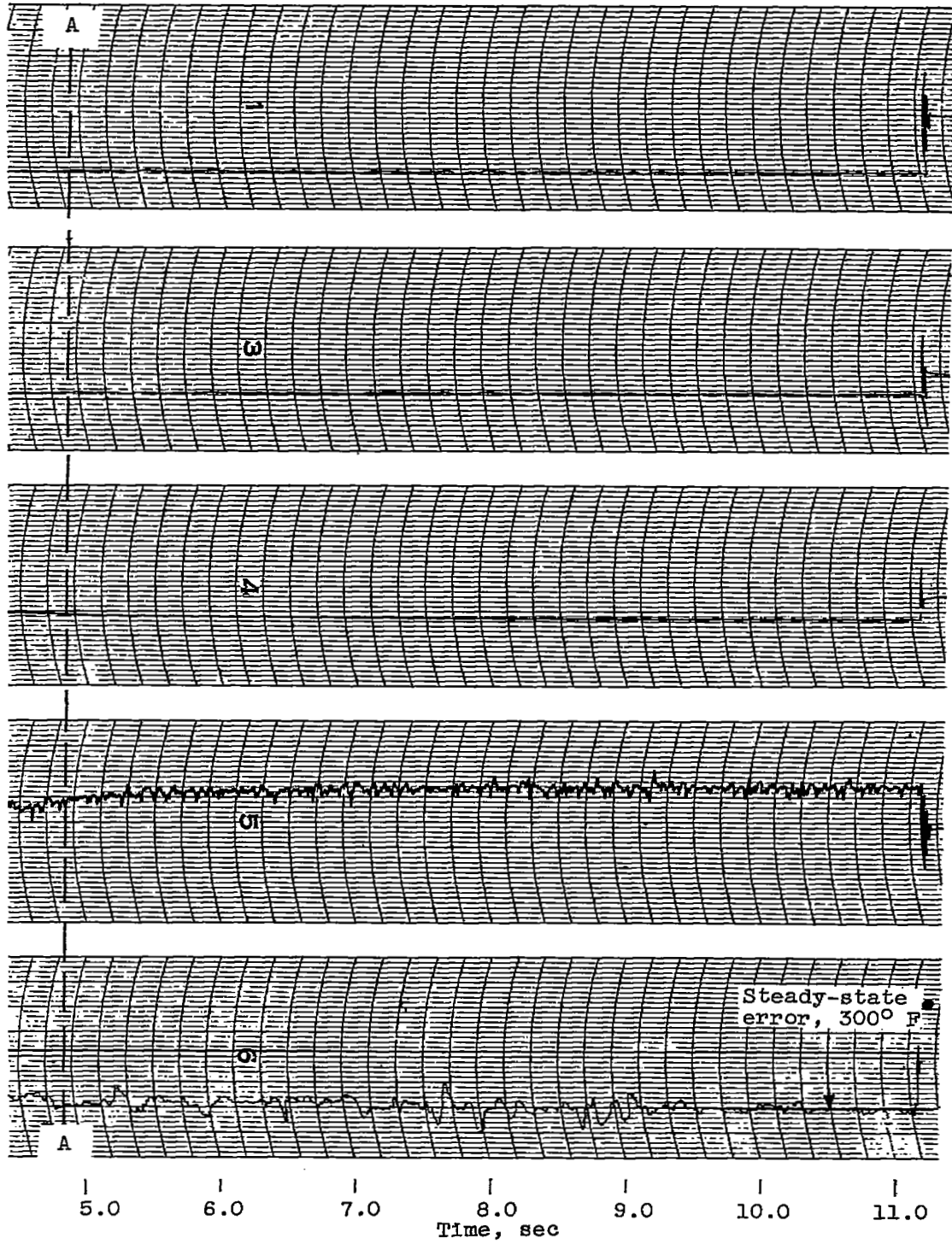


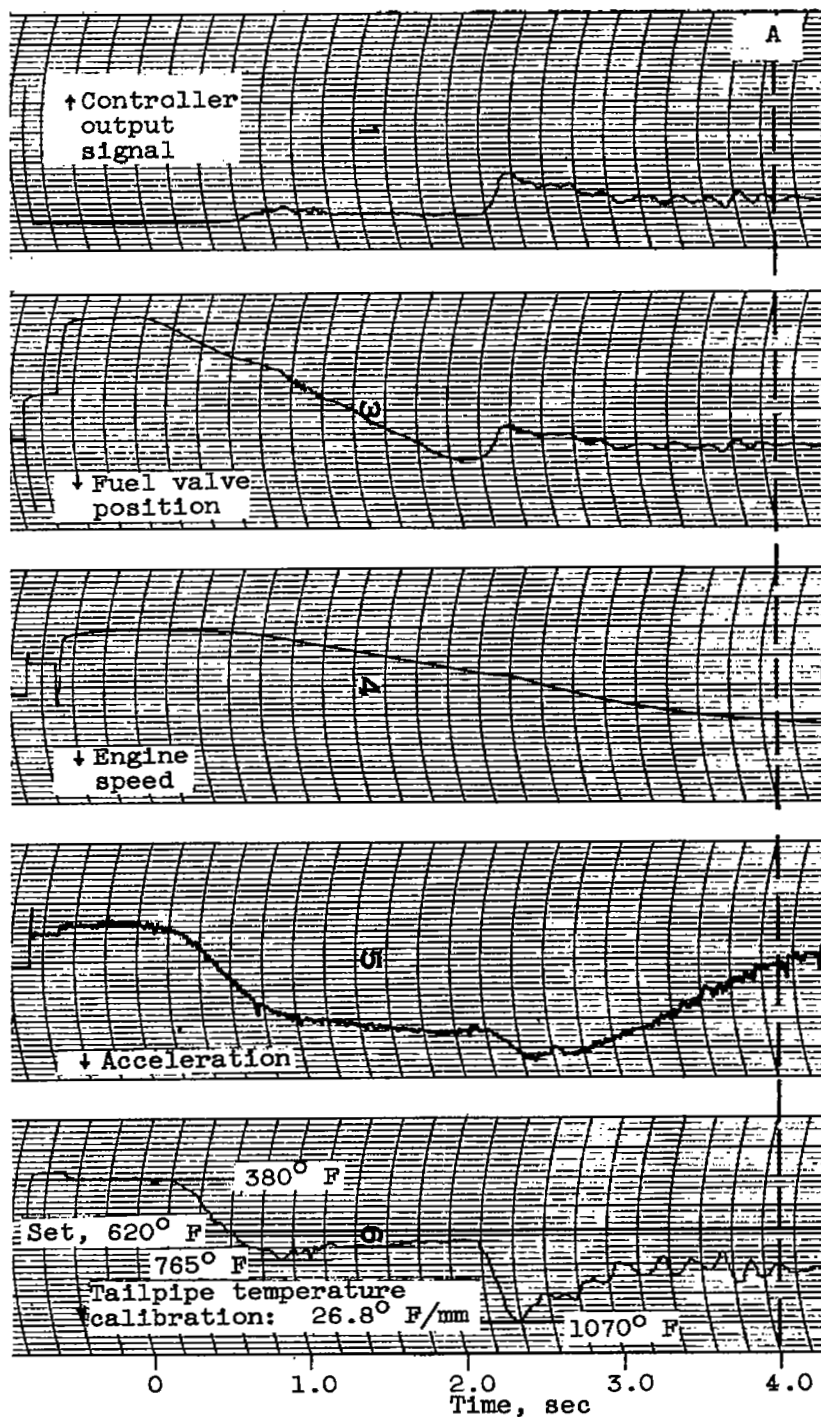


(a) Proportional control gain, 3.25.

Figure 15. - Transient data with proportional control action.

3974

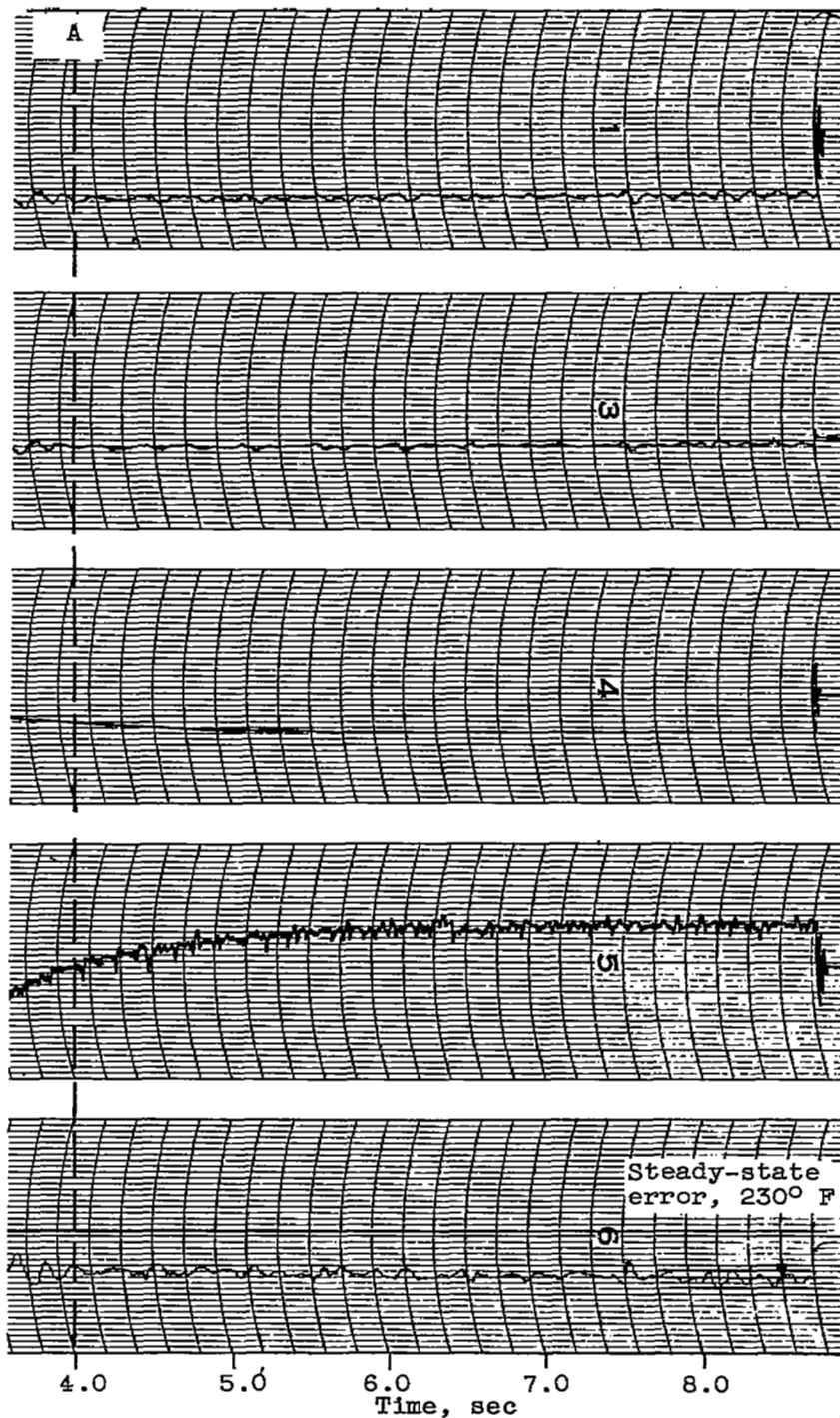


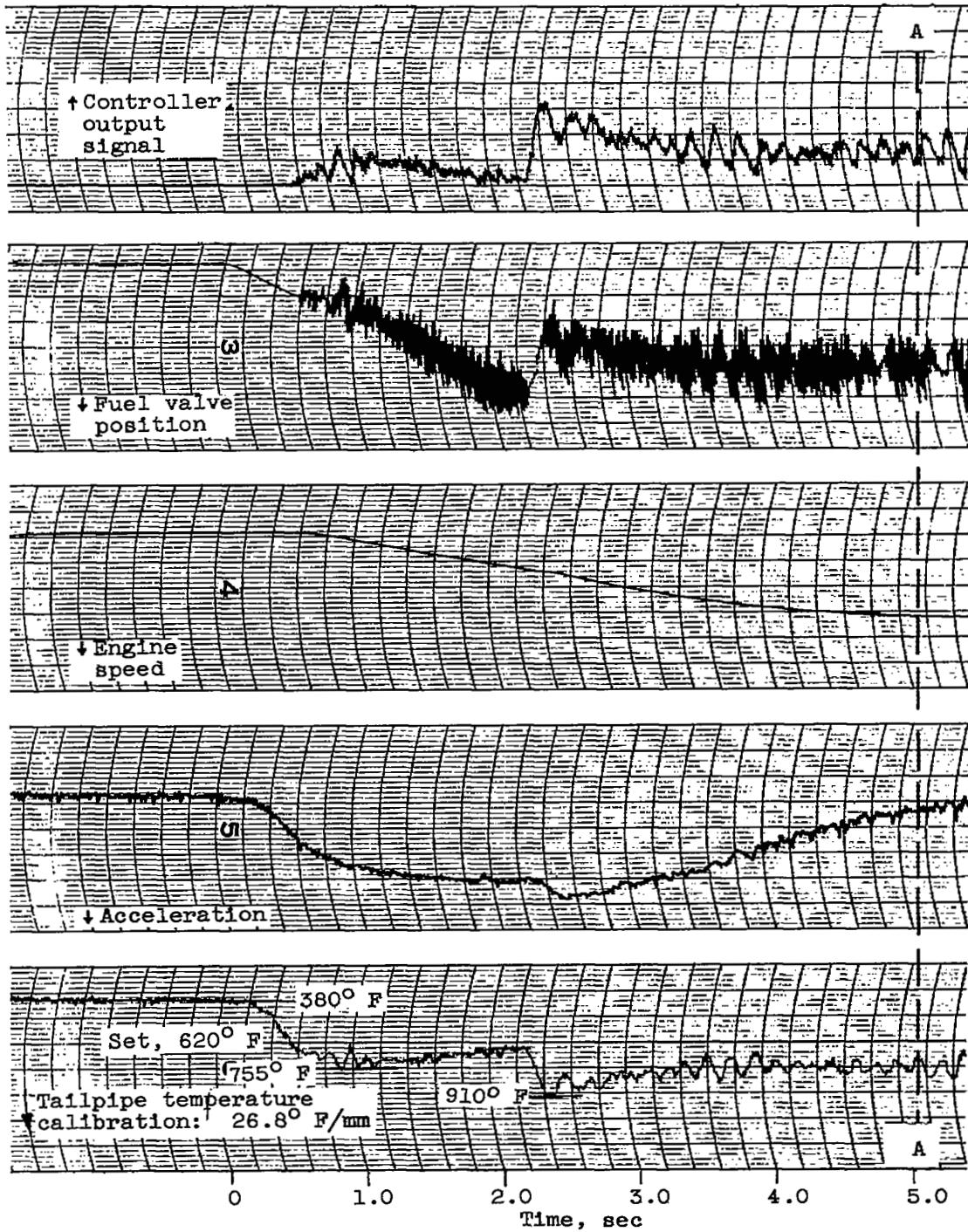


(b) Proportional control gain, 13.0.

Figure 15. - Continued. Transient data with proportional control action.

3974



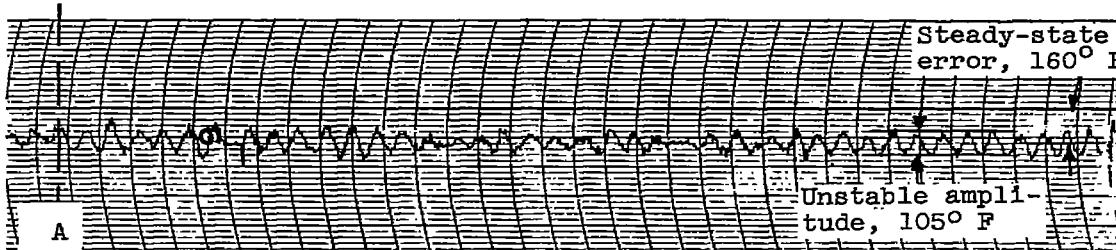
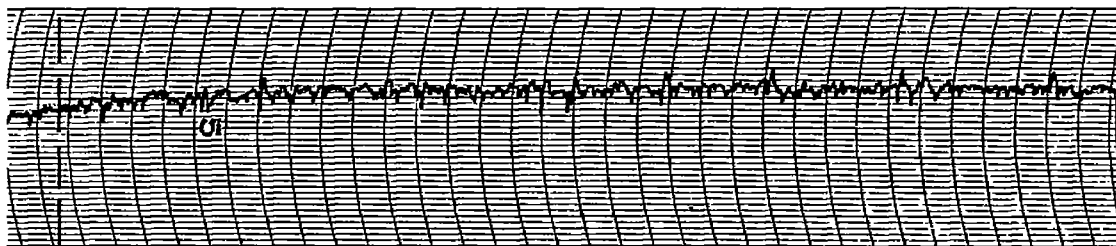
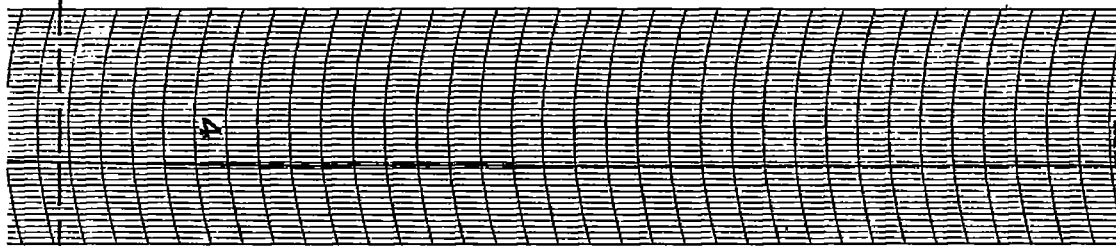
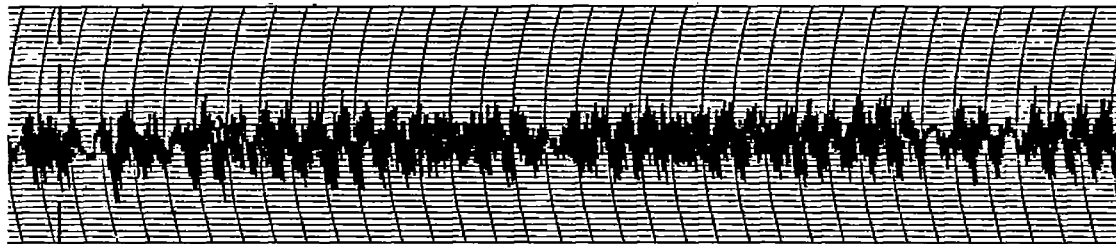
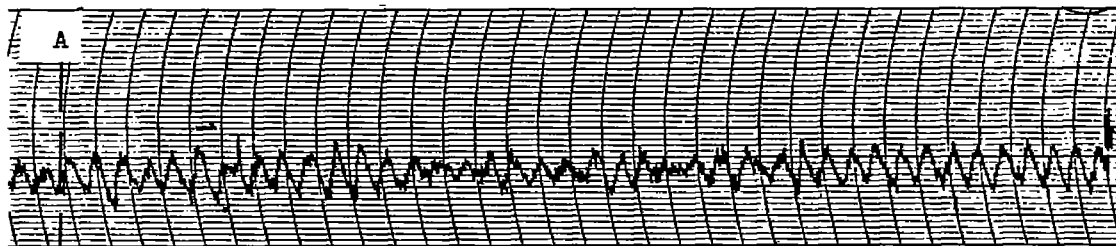


(c) Proportional control gain, 39.0.

Figure 15. - Continued. Transient data with proportional control action.

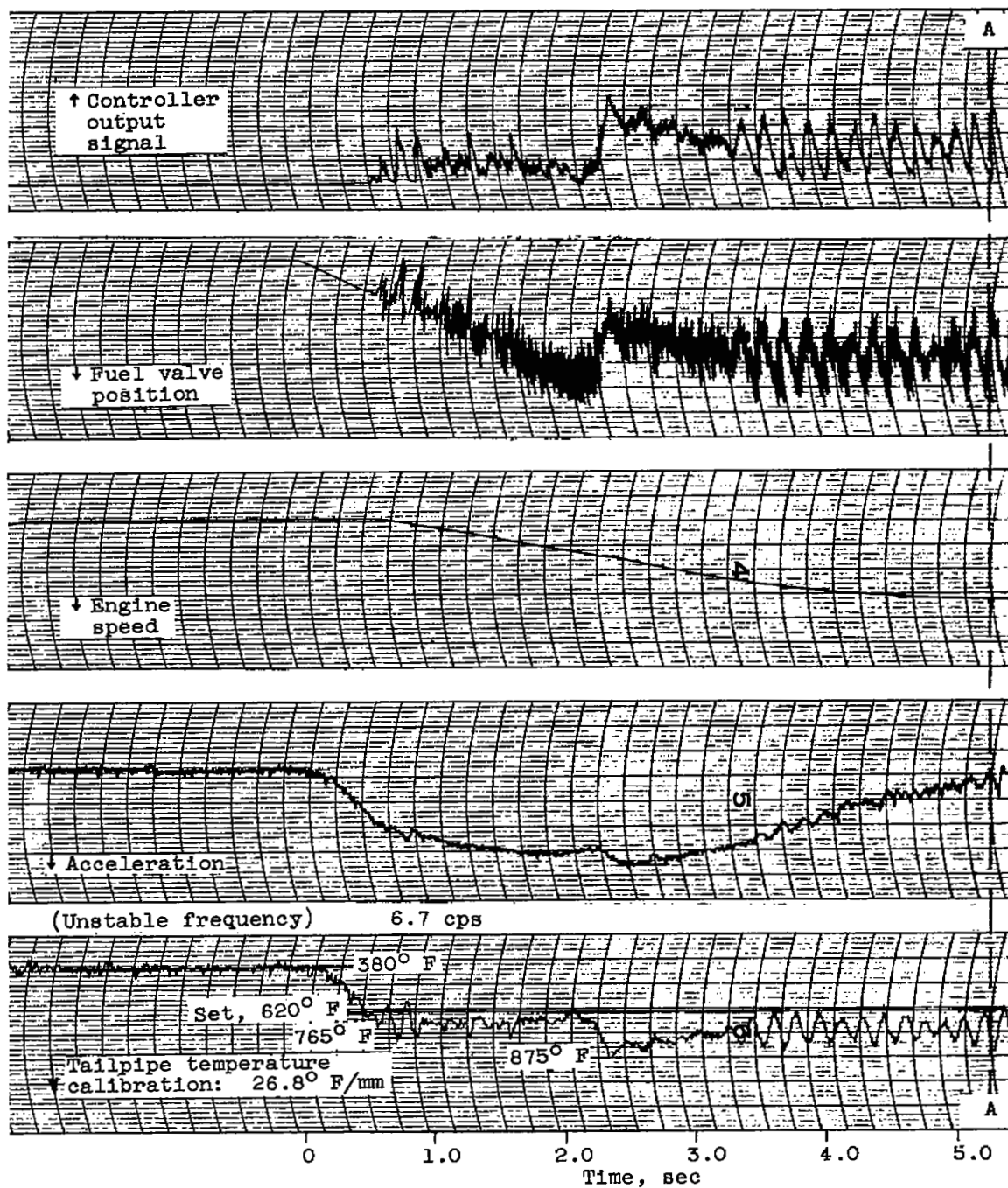
5974

CD-6



5.0 6.0 7.0 8.0 9.0 10.0 11.0  
Time, sec

~~CONFIDENTIAL~~

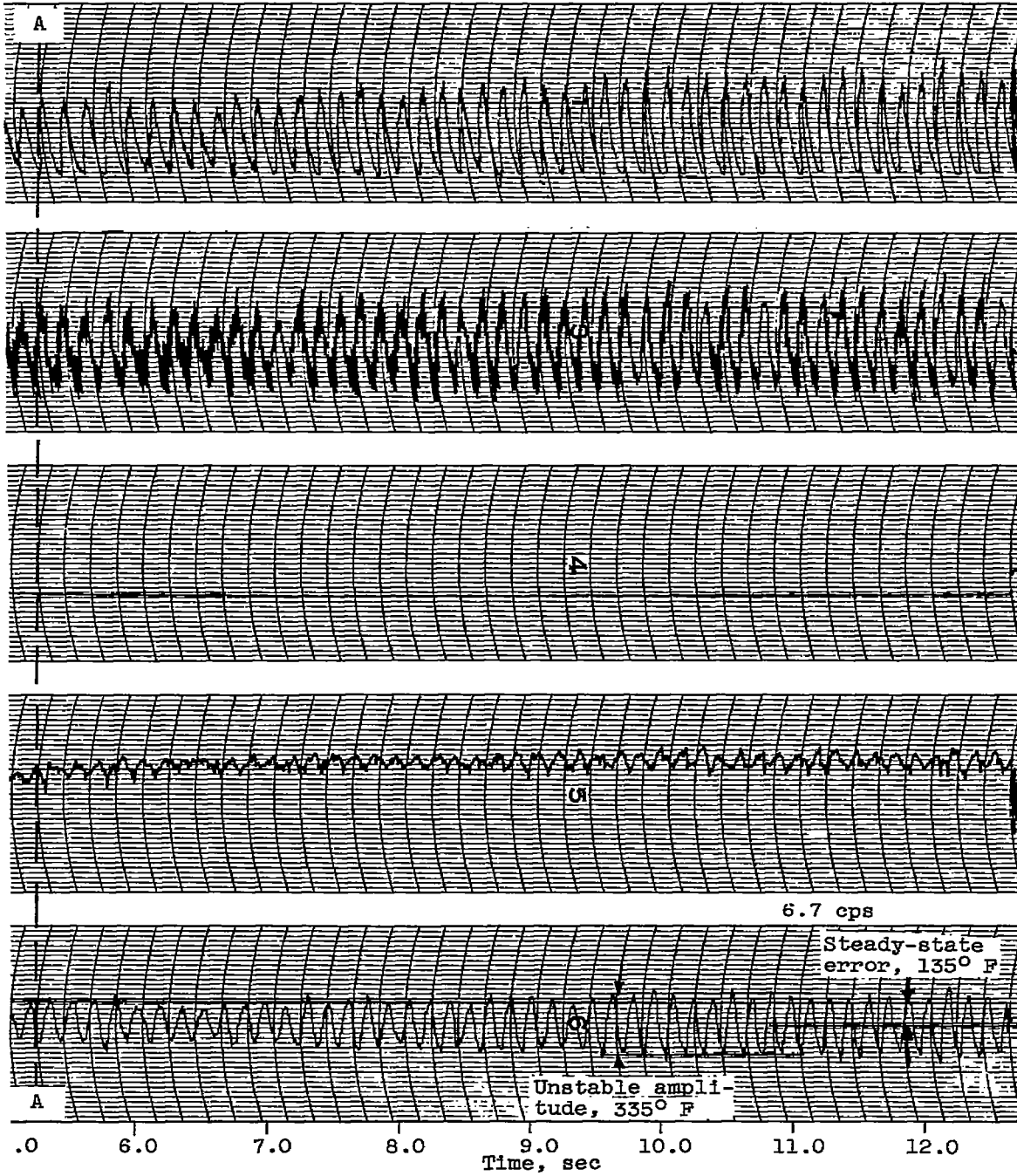


(d) Proportional control gain, 45.5.

Figure 15. - Concluded. Transient data with proportional control action.

3974

CD-6 back



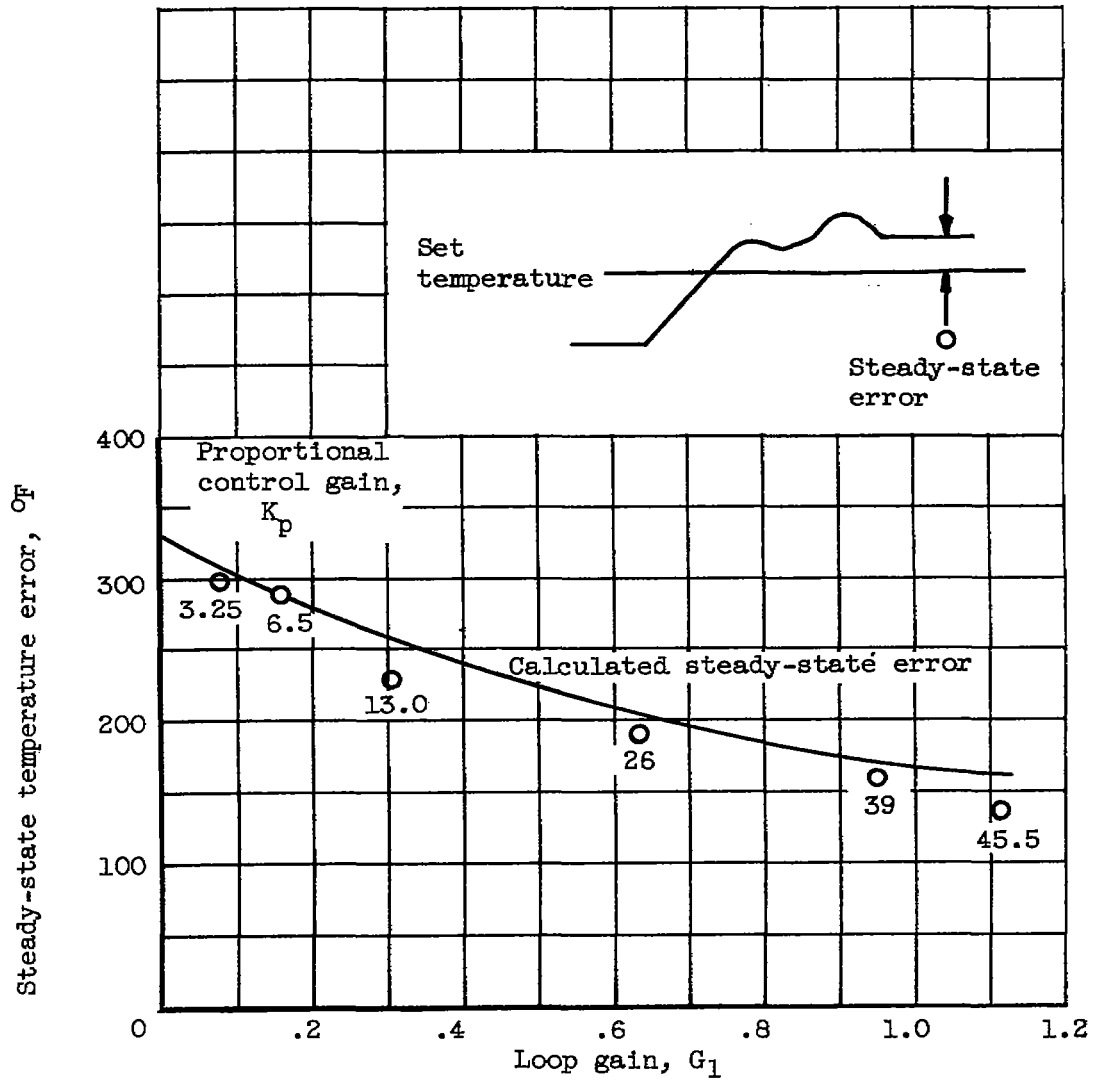
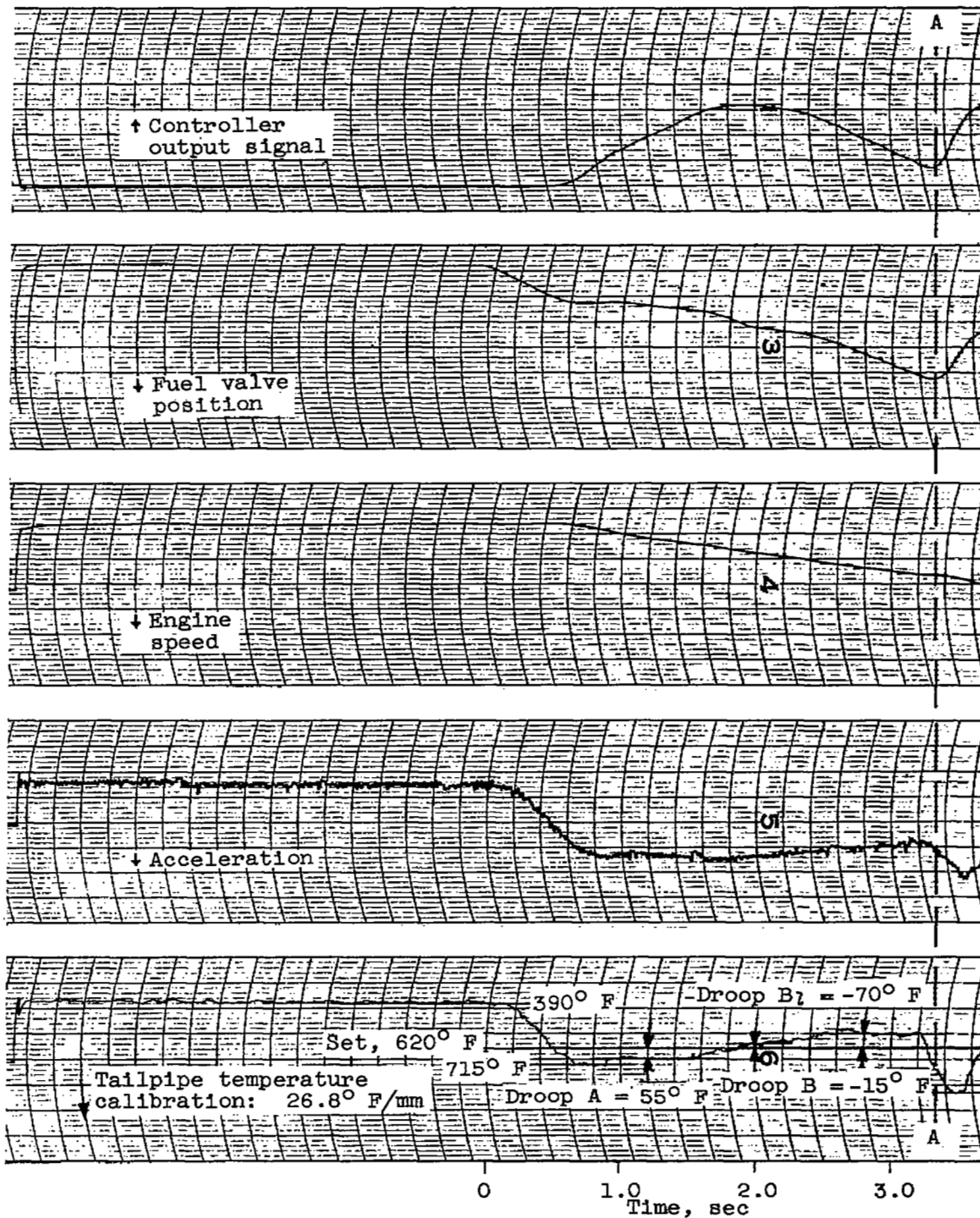


Figure 16. - Variation of proportional-control steady-state temperature error with loop gain.

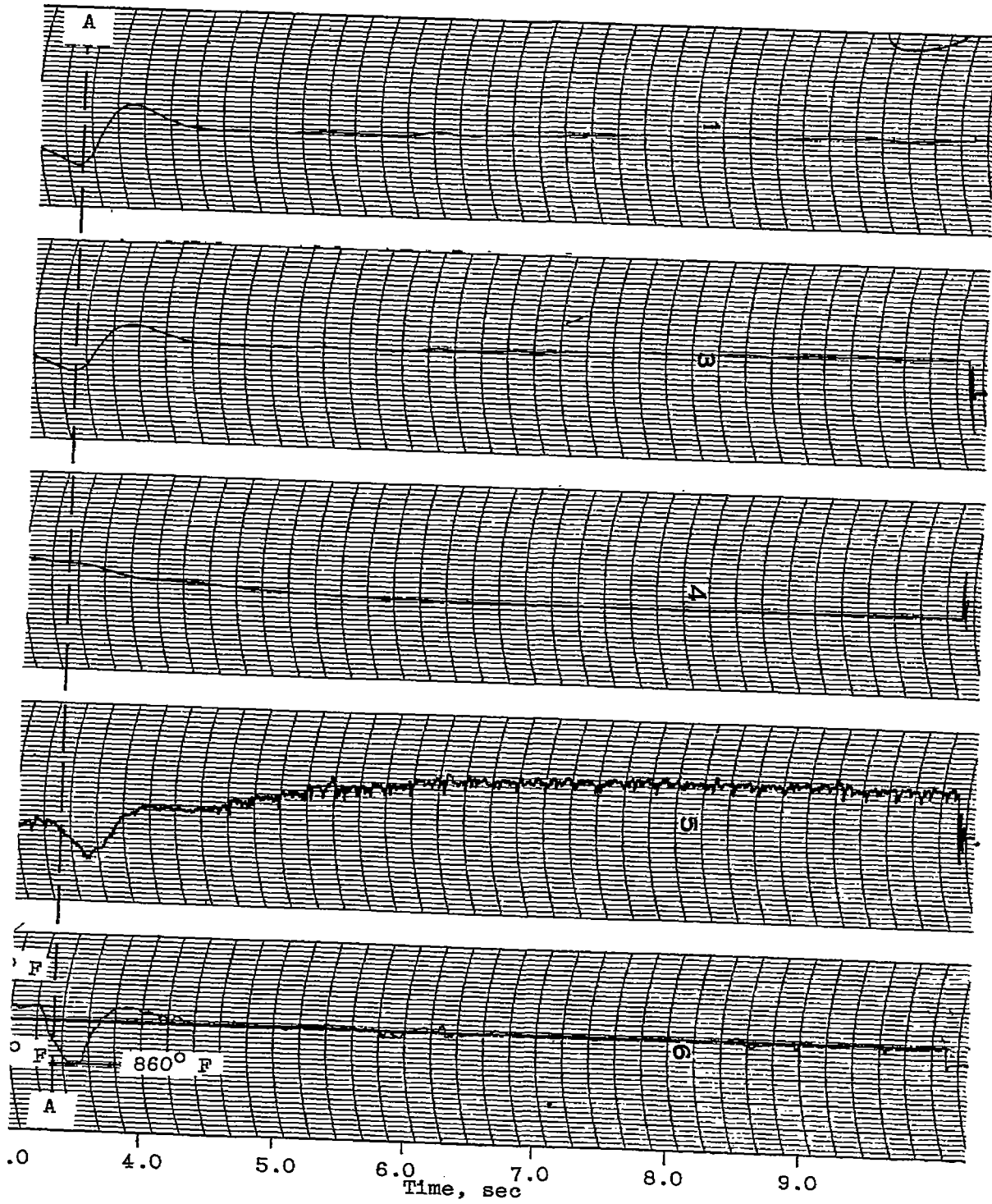
3974

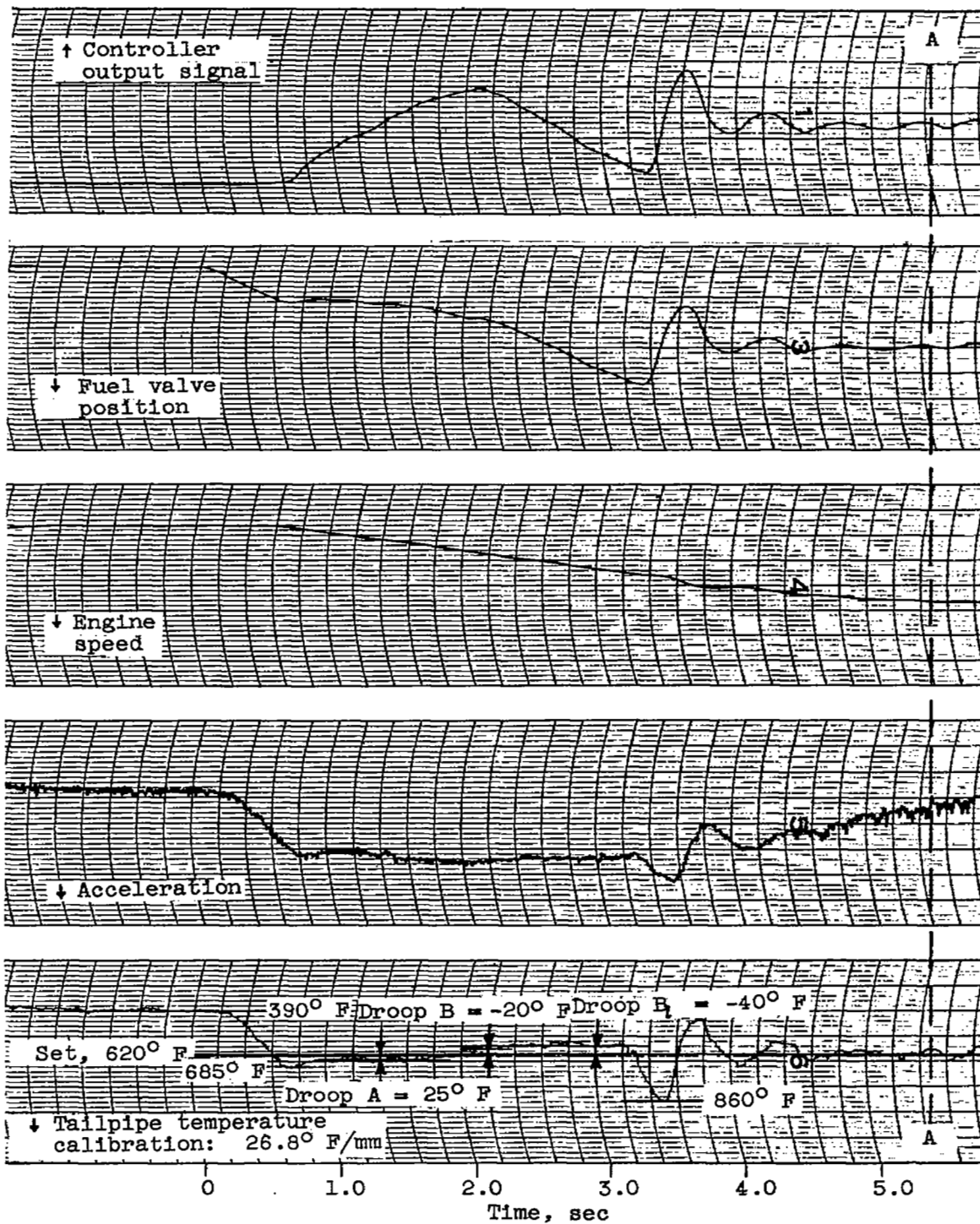


(a) Integral control gain, 130.

Figure 17. - Transient data with integral control action.

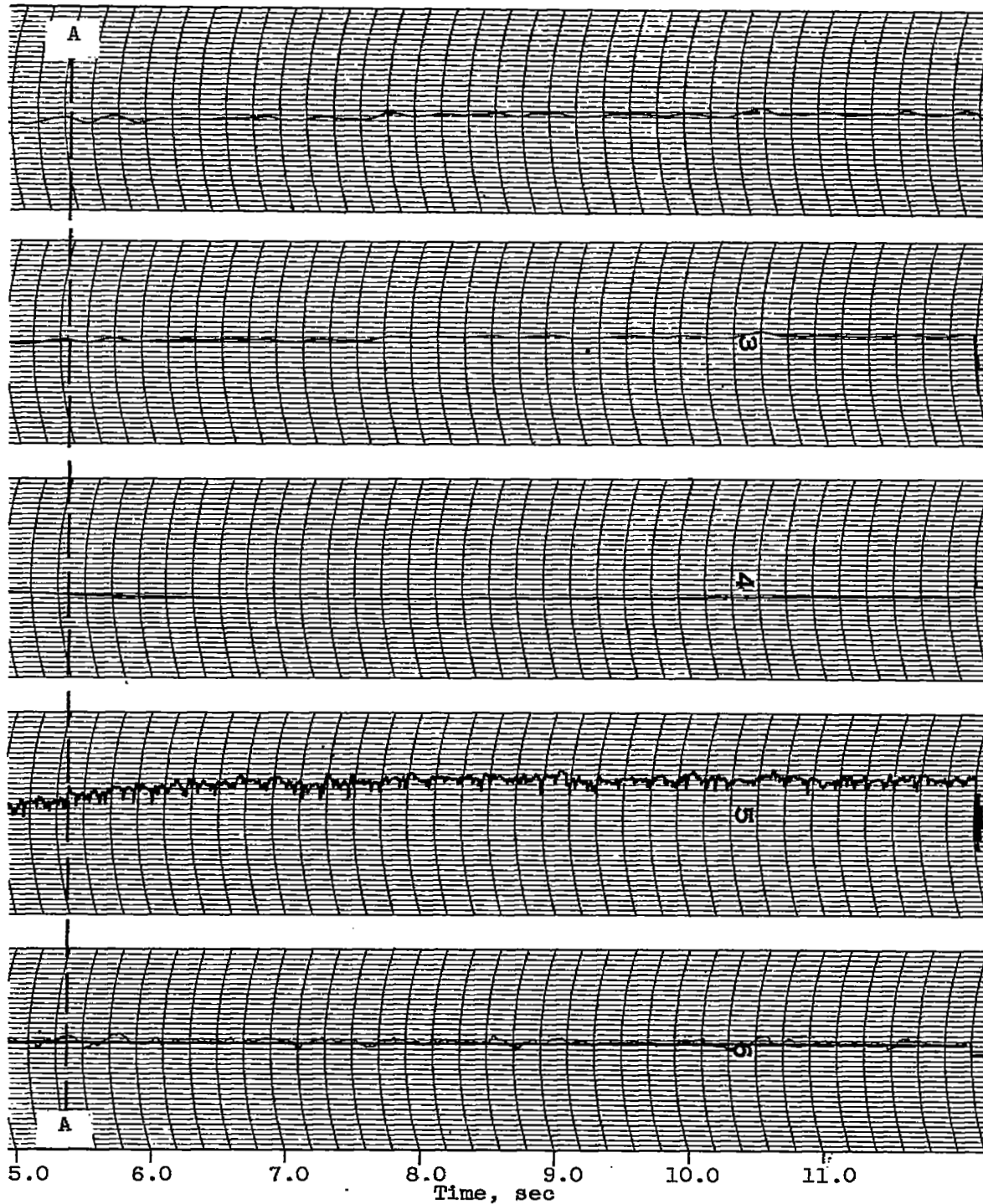
3974





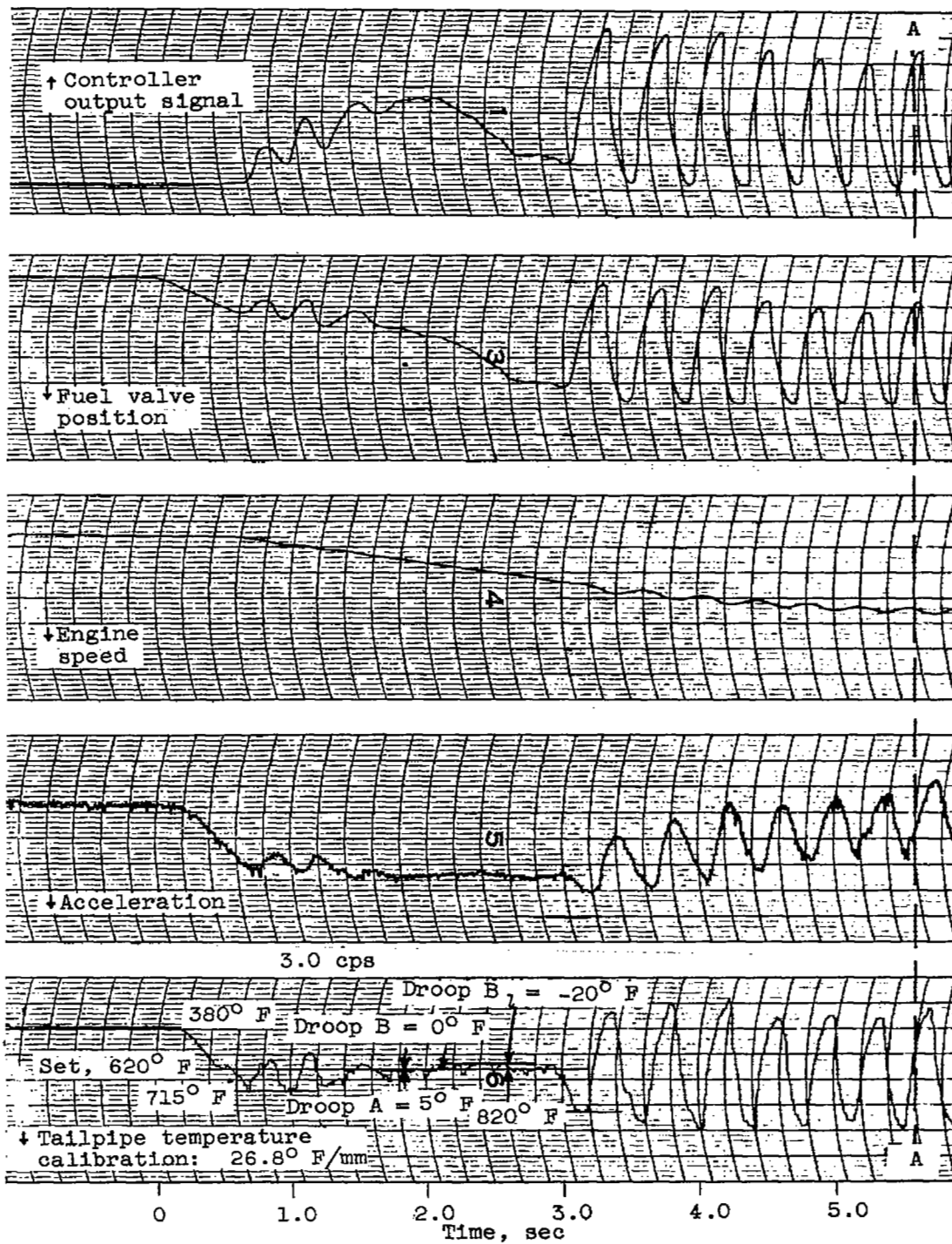
(b) Integral control gain, 260.

Figure 17. - Continued. Transient data with integral control action.



35/4

35

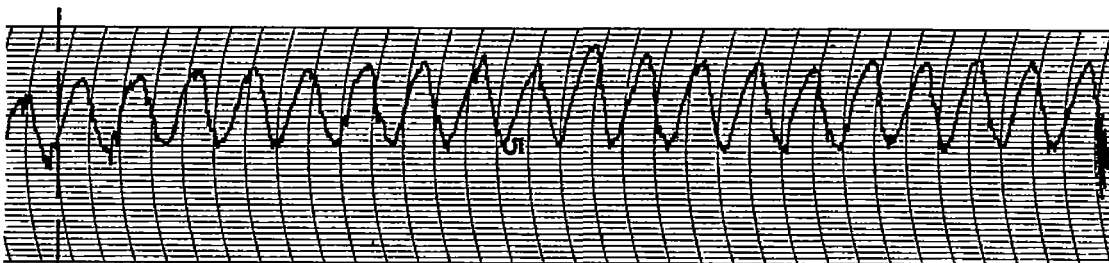
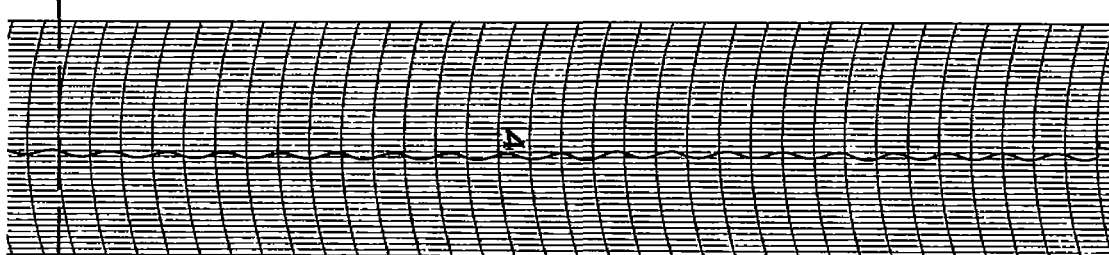
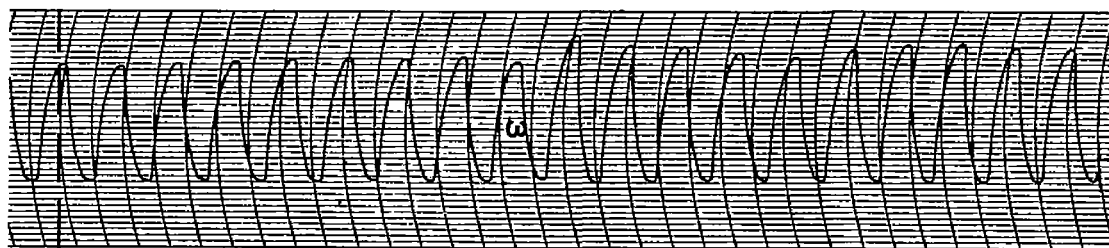


(c) Integral control gain, 520.

Figure 17. - Concluded. Transient data with integral control action.

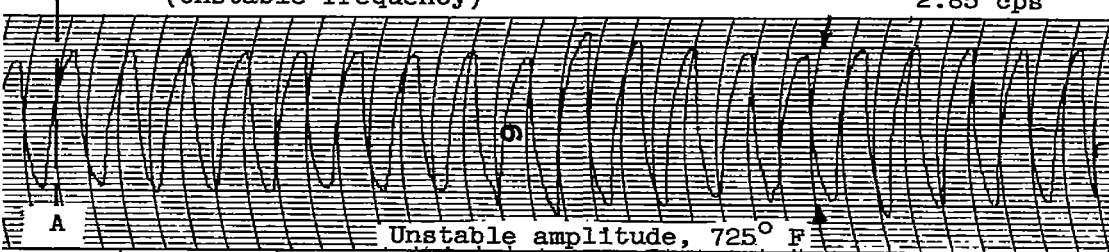
3974

CD-7 bac.



(Unstable frequency)

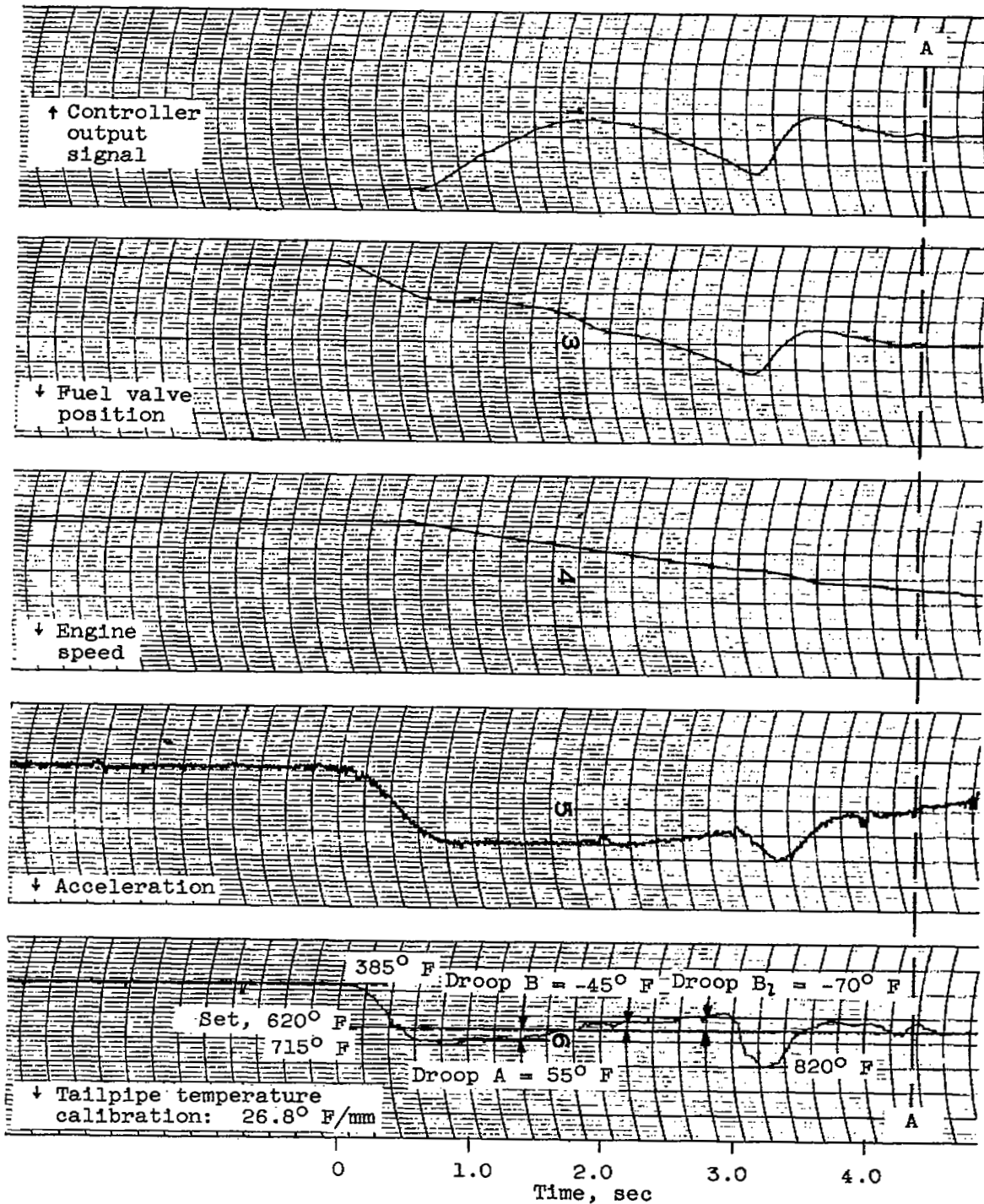
2.85 cps



Unstable amplitude, 725° F

6.0 7.0 8.0 9.0 10.0 11.0 12.0  
Time, sec

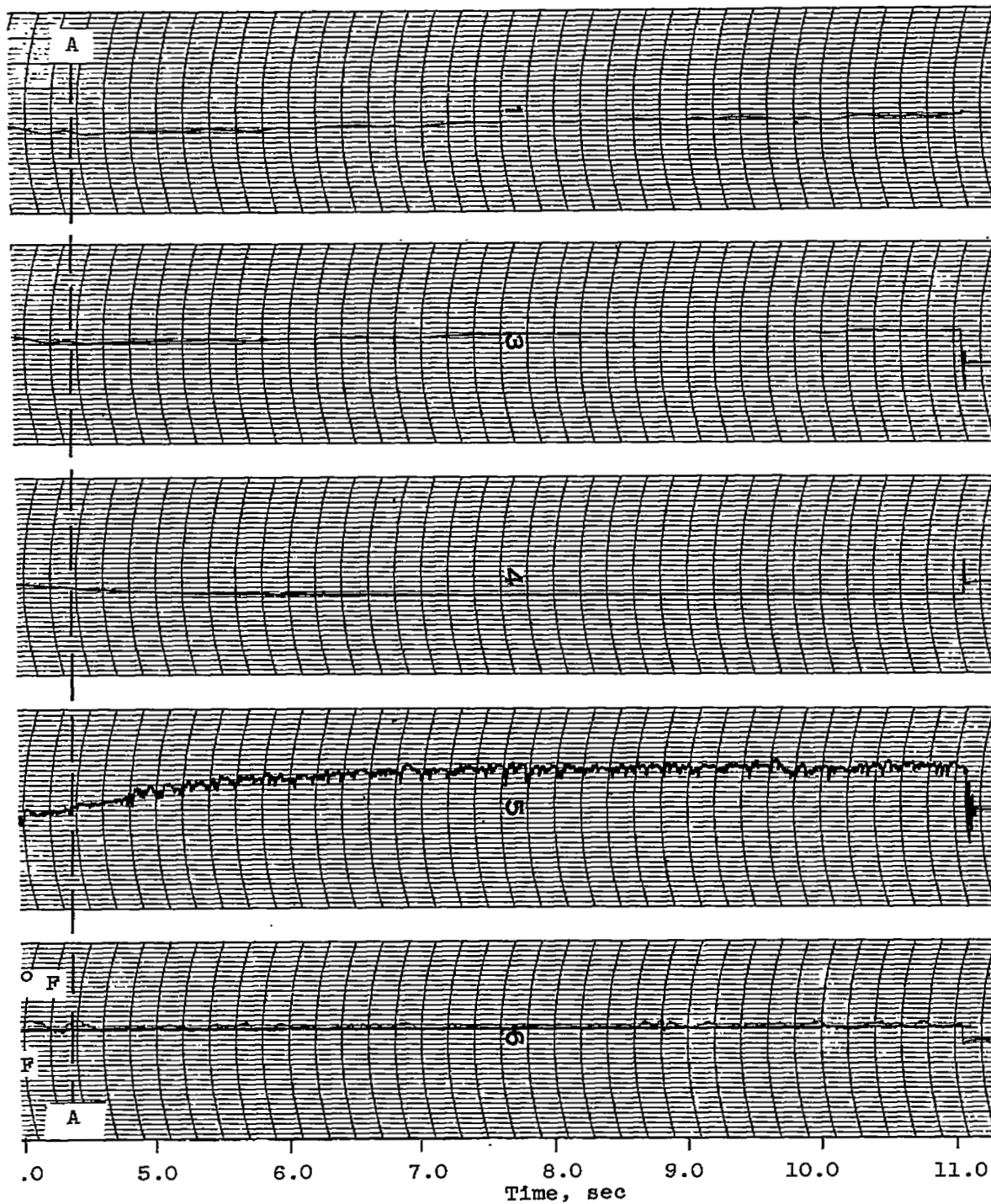
[Redacted]

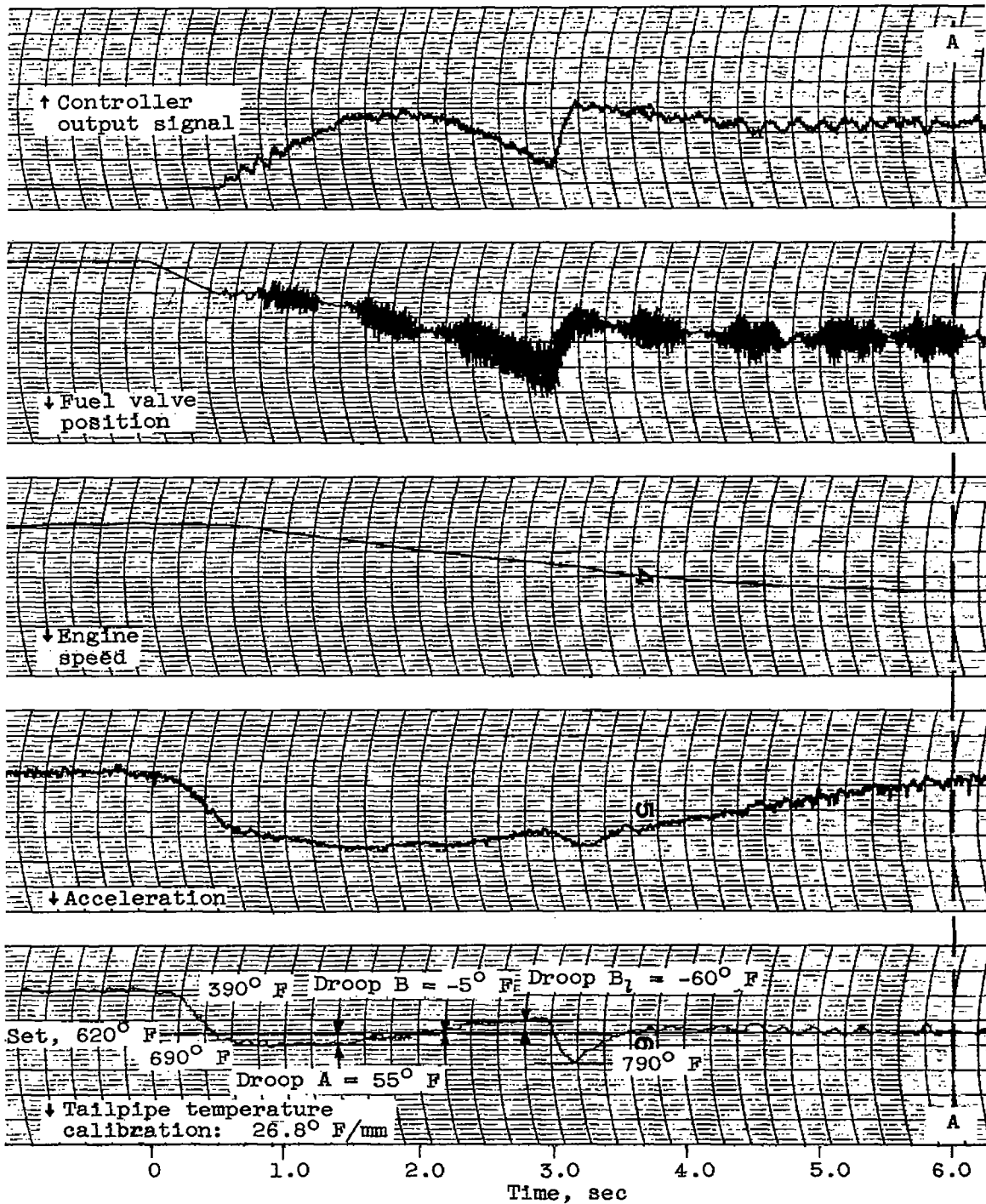


(a) Proportional control gain, 3.25.

Figure 18. - Transient data for proportional-plus-integral control action. Integral control gain, 130.

3974

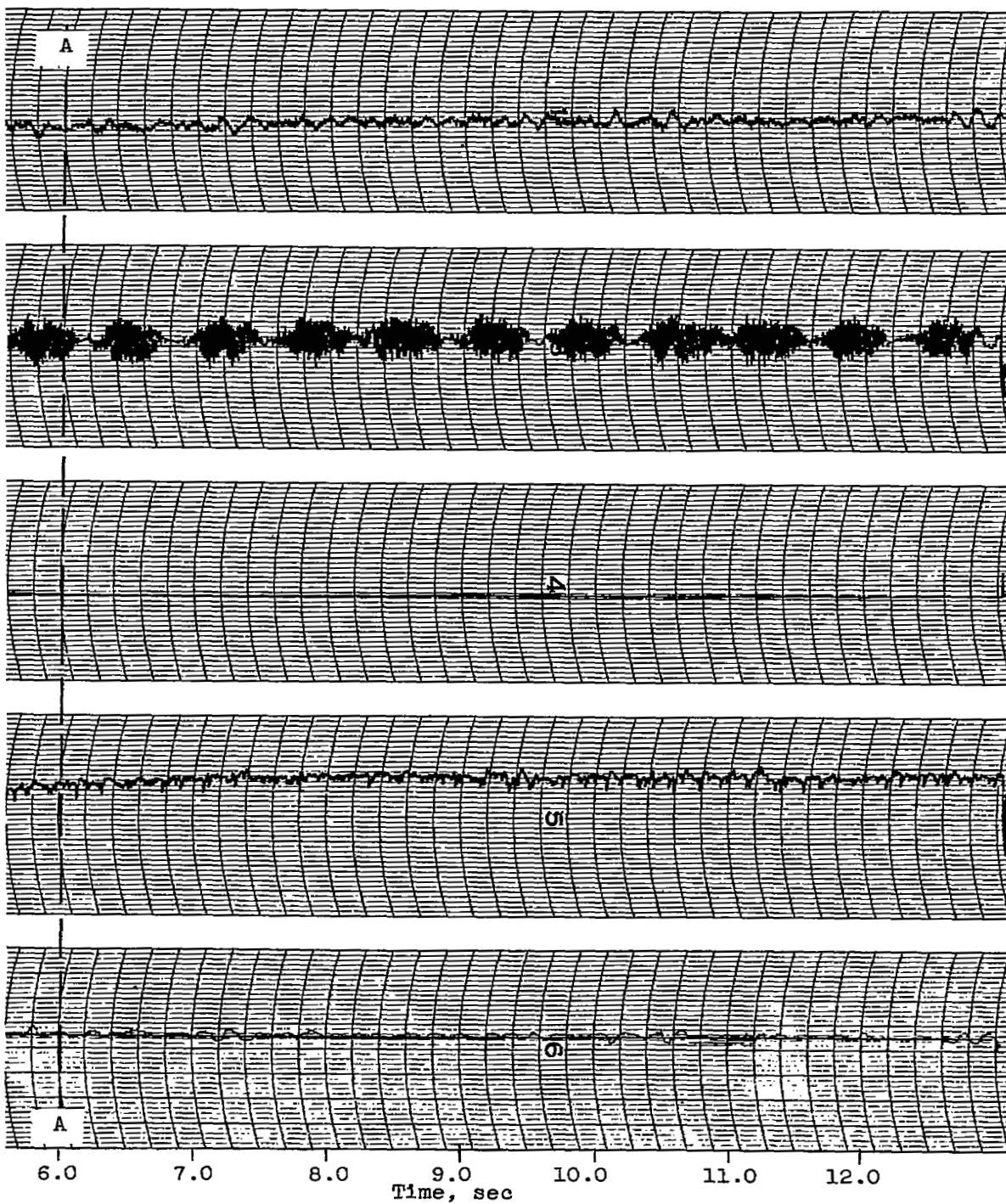


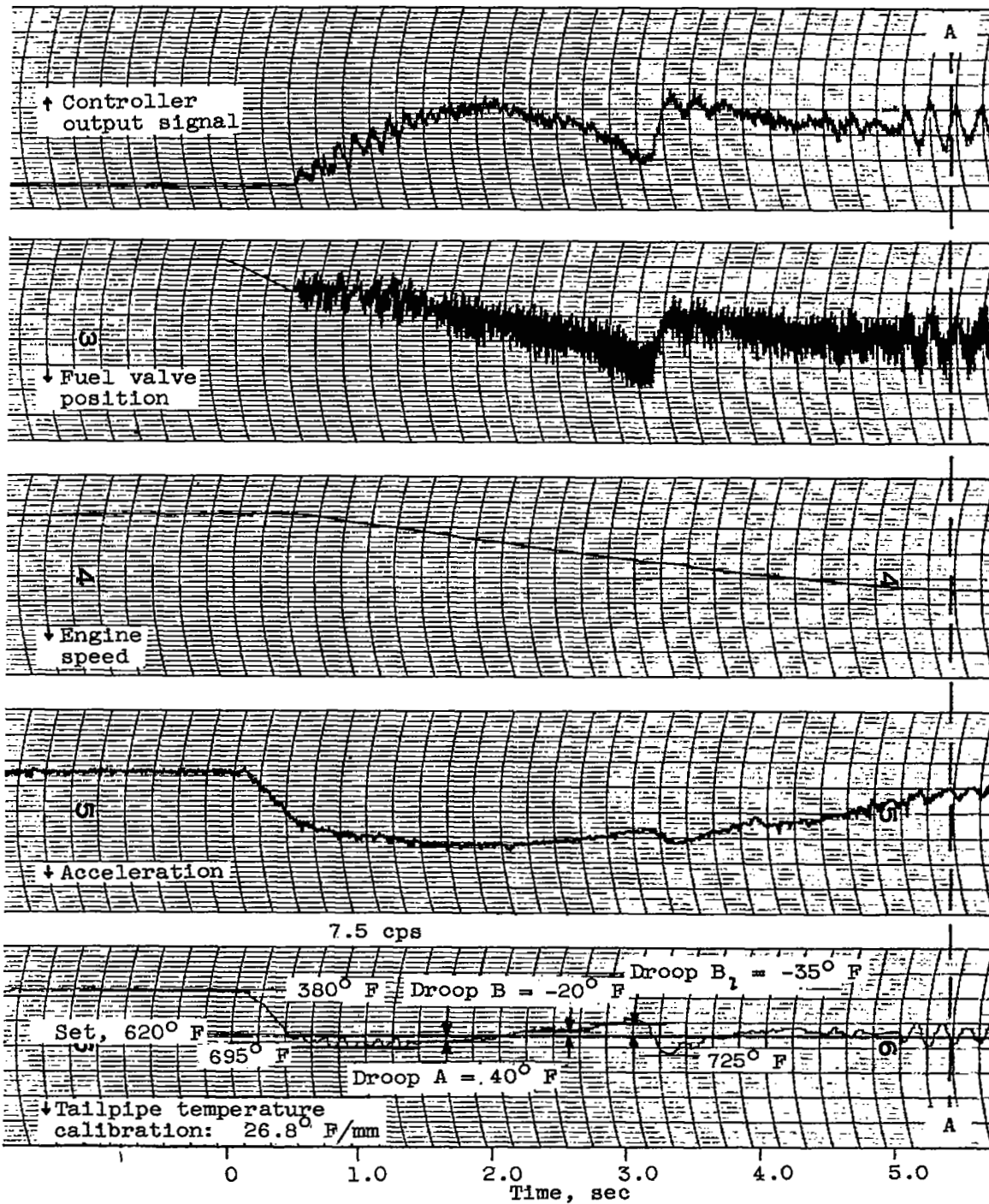


(b) Proportional control gain, 26.0.

Figure 18. - Continued. Transient data for proportional-plus-integral control action. Integral control gain, 130.

3974

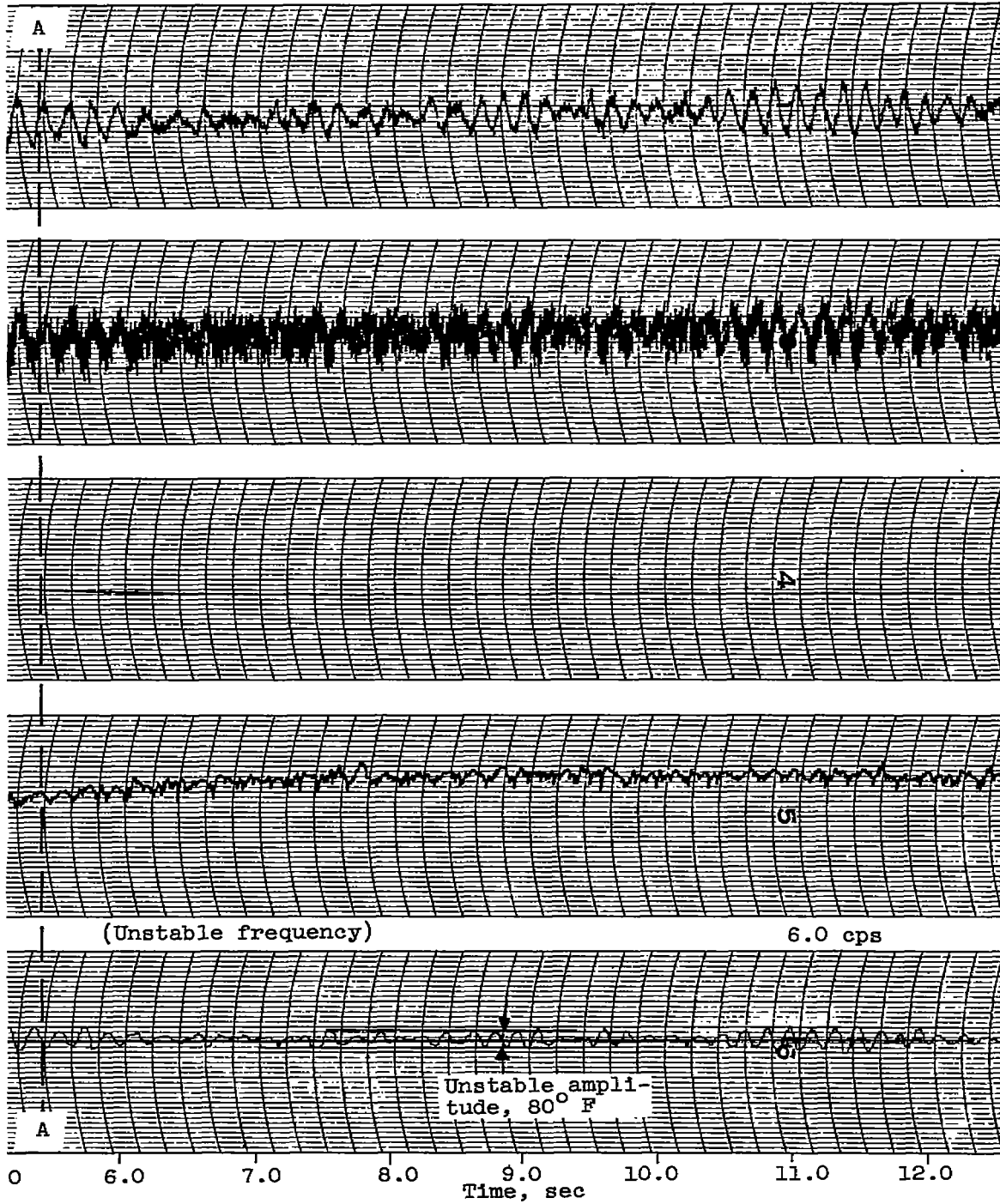


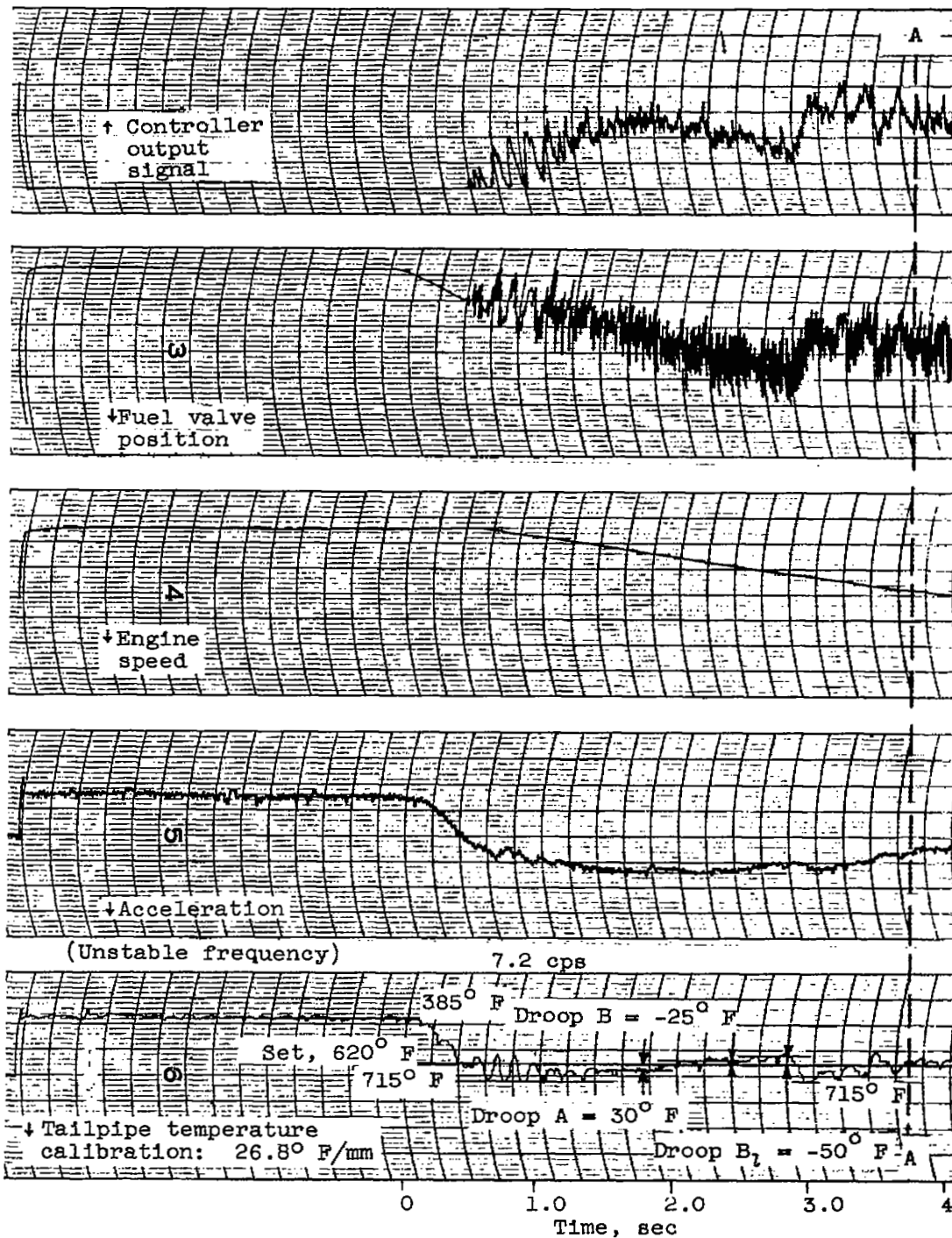


(c) Proportional control gain, 39.

Figure 18. - Continued. Transient data for proportional-plus-integral control action. Integral control gain, 130.

3974



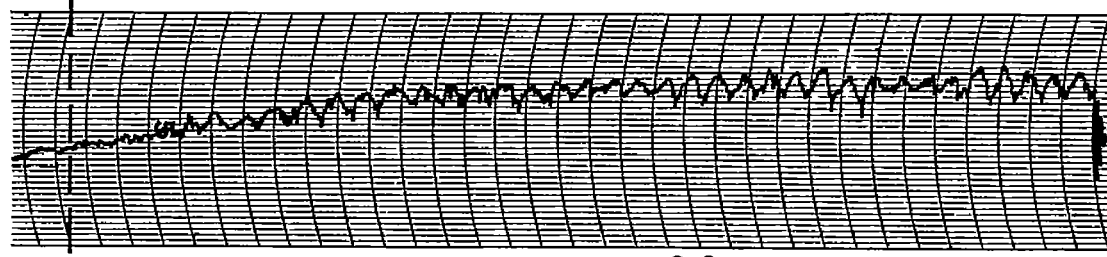
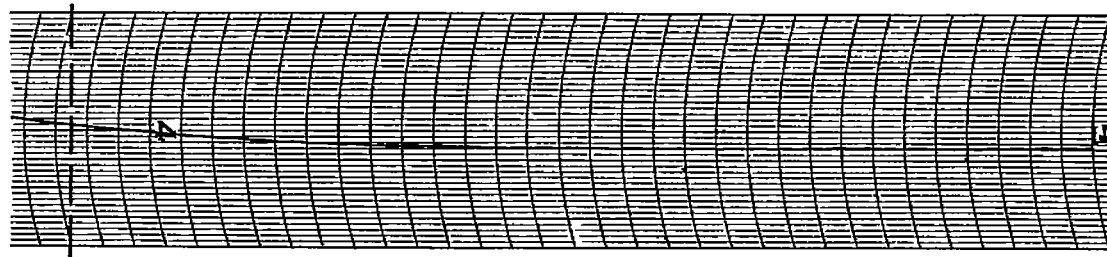
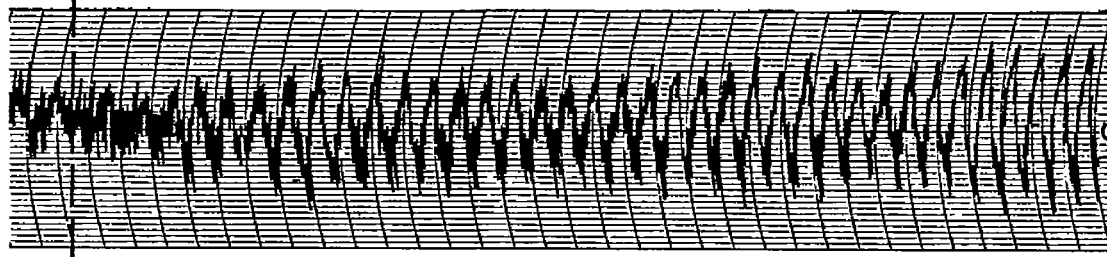
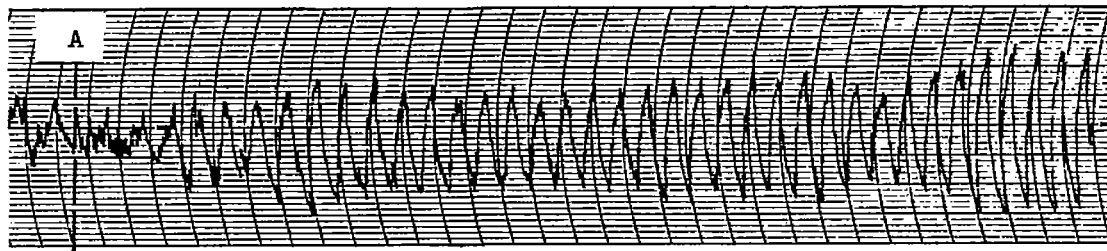


(d) Proportional control gain, 45.5.

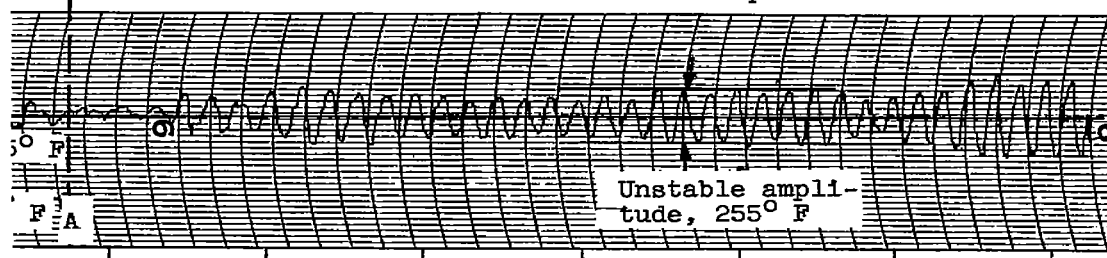
Figure 18. - Concluded. Transient data for proportional-plus-integral control action. Integral control gain, 130.

~~CONFIDENTIAL~~

5974



6.0 cps



Unstable amplitude, 255° F

4.0 5.0 6.0 7.0 8.0 9.0 10.0  
Time, sec

~~CONFIDENTIAL~~

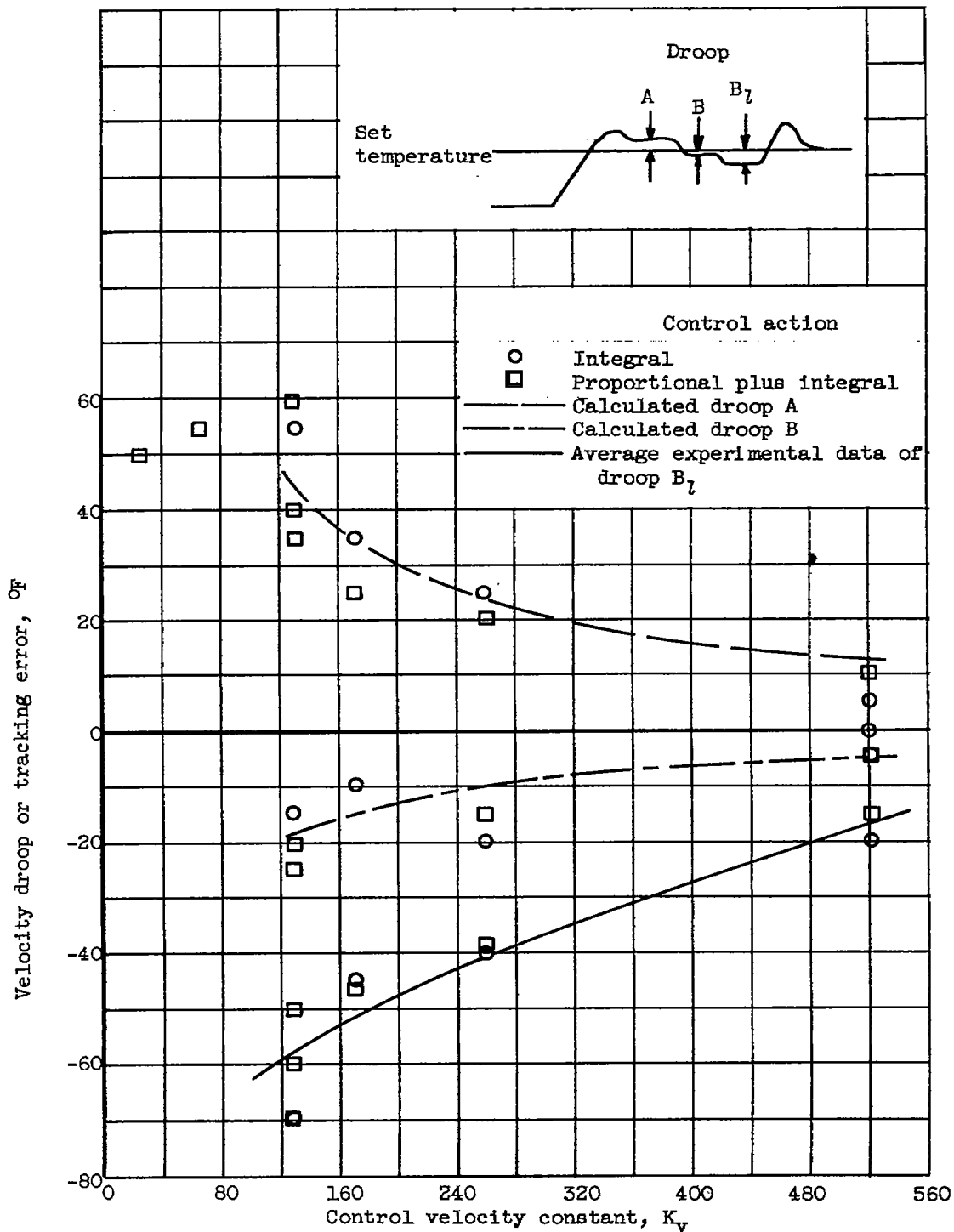
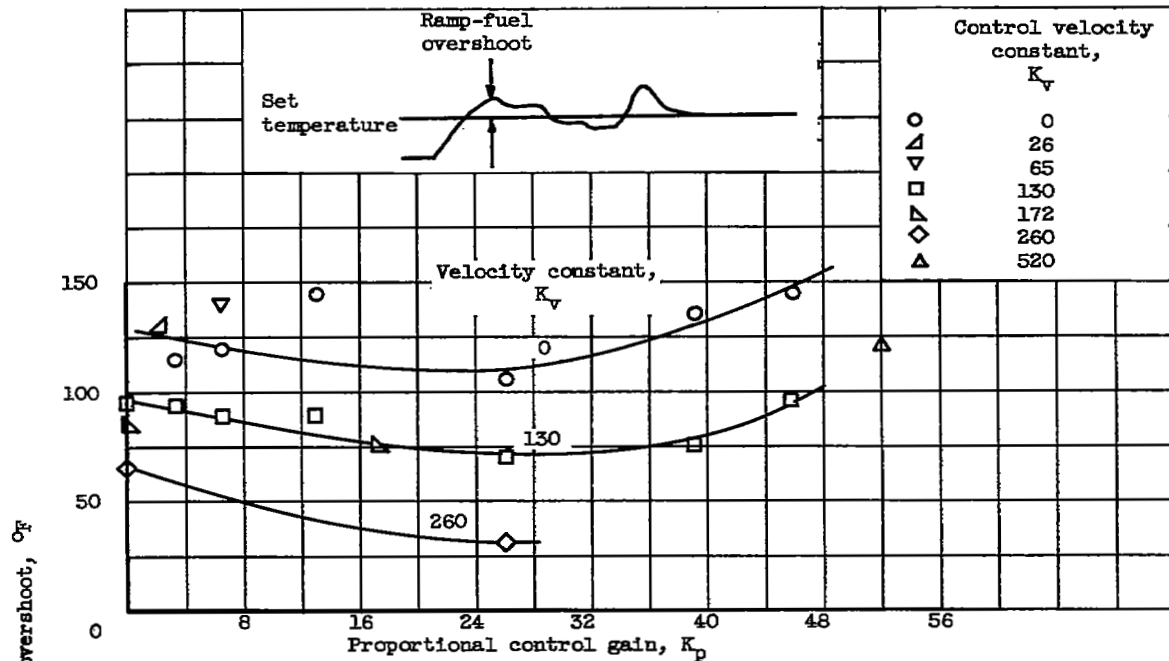
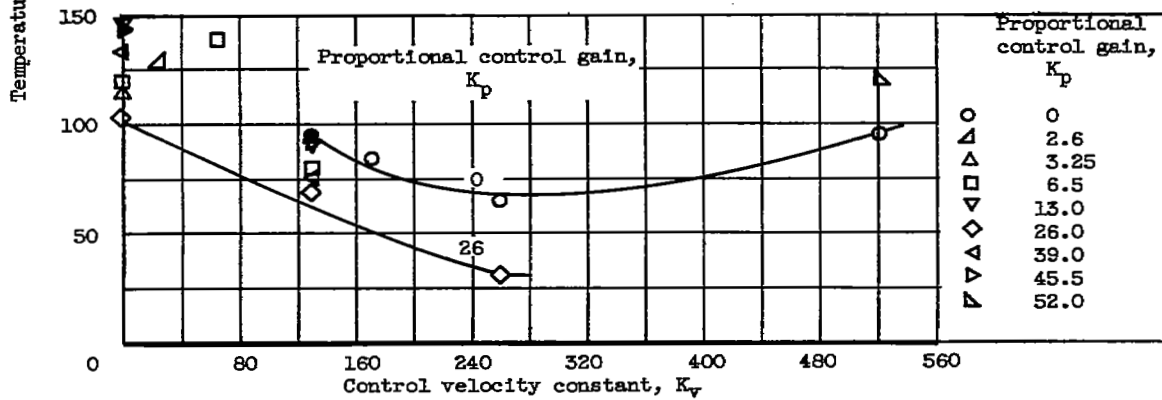


Figure 19. - Variation of velocity error with control velocity constant for integral and proportional-plus integral control action.

3974

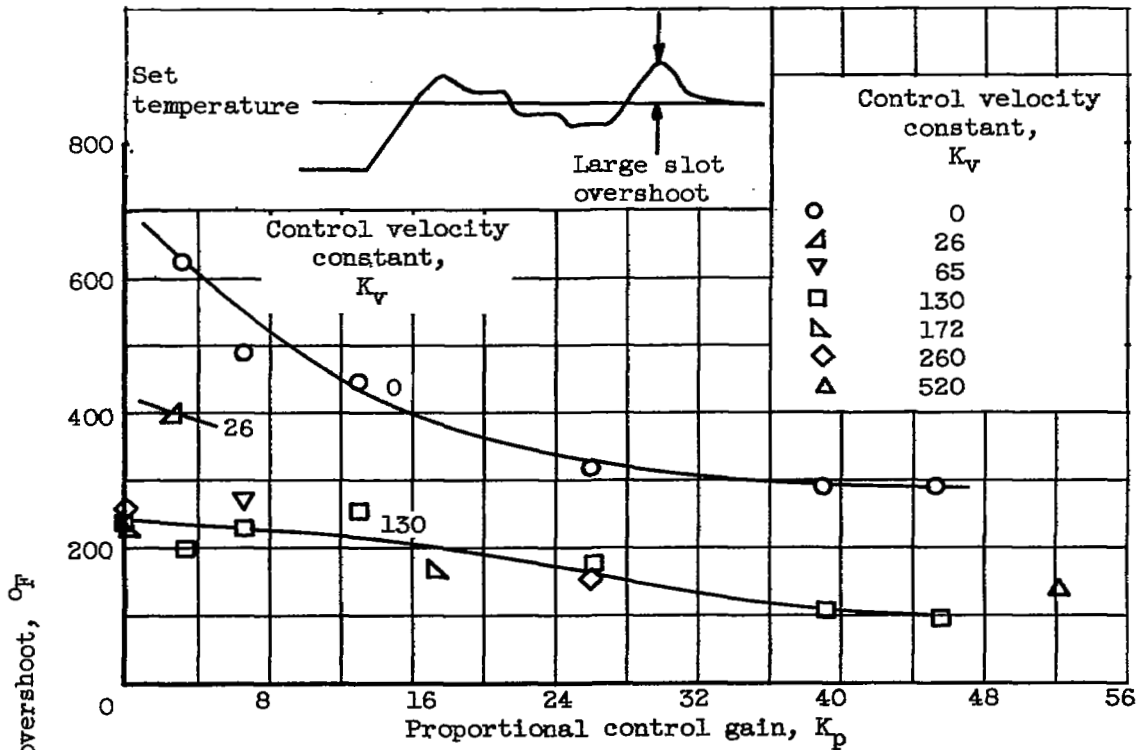


(a) For variations of proportional control gain.

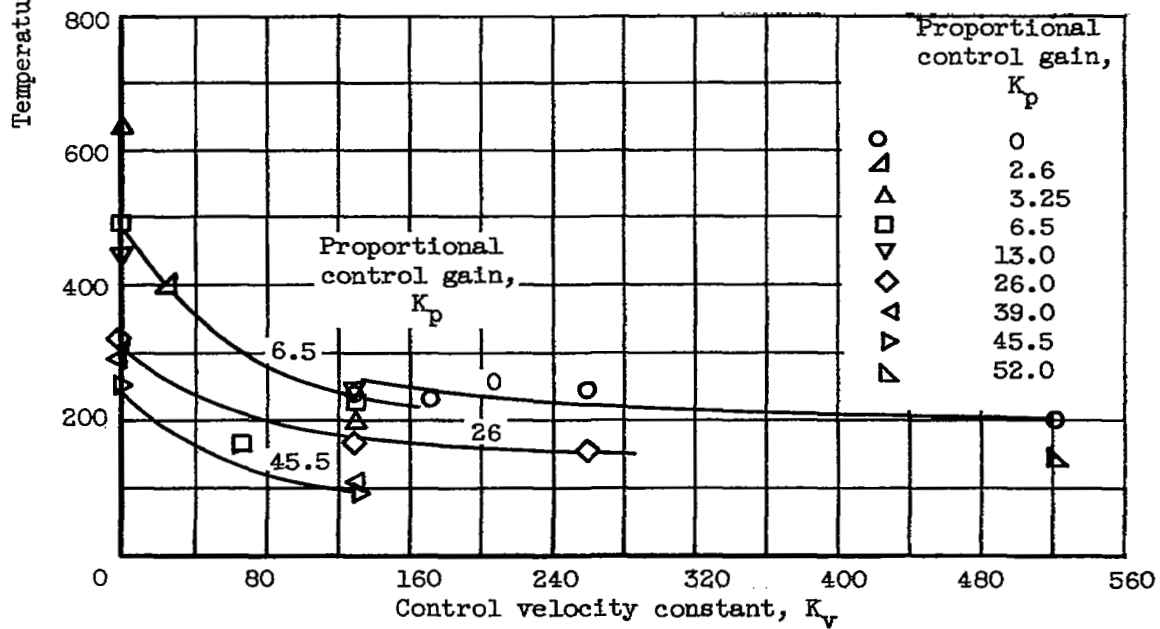


(b) For variations of control velocity constant.

Figure 20. - Temperature overshoot data resulting from 35 percent rated fuel flow per second ramp input initiated at  $62\frac{1}{2}$  percent rated engine speed.



(a) With proportional control gain.



(b) With control velocity constant.

Figure 21. - Variation of large-slot temperature overshoot.

3974

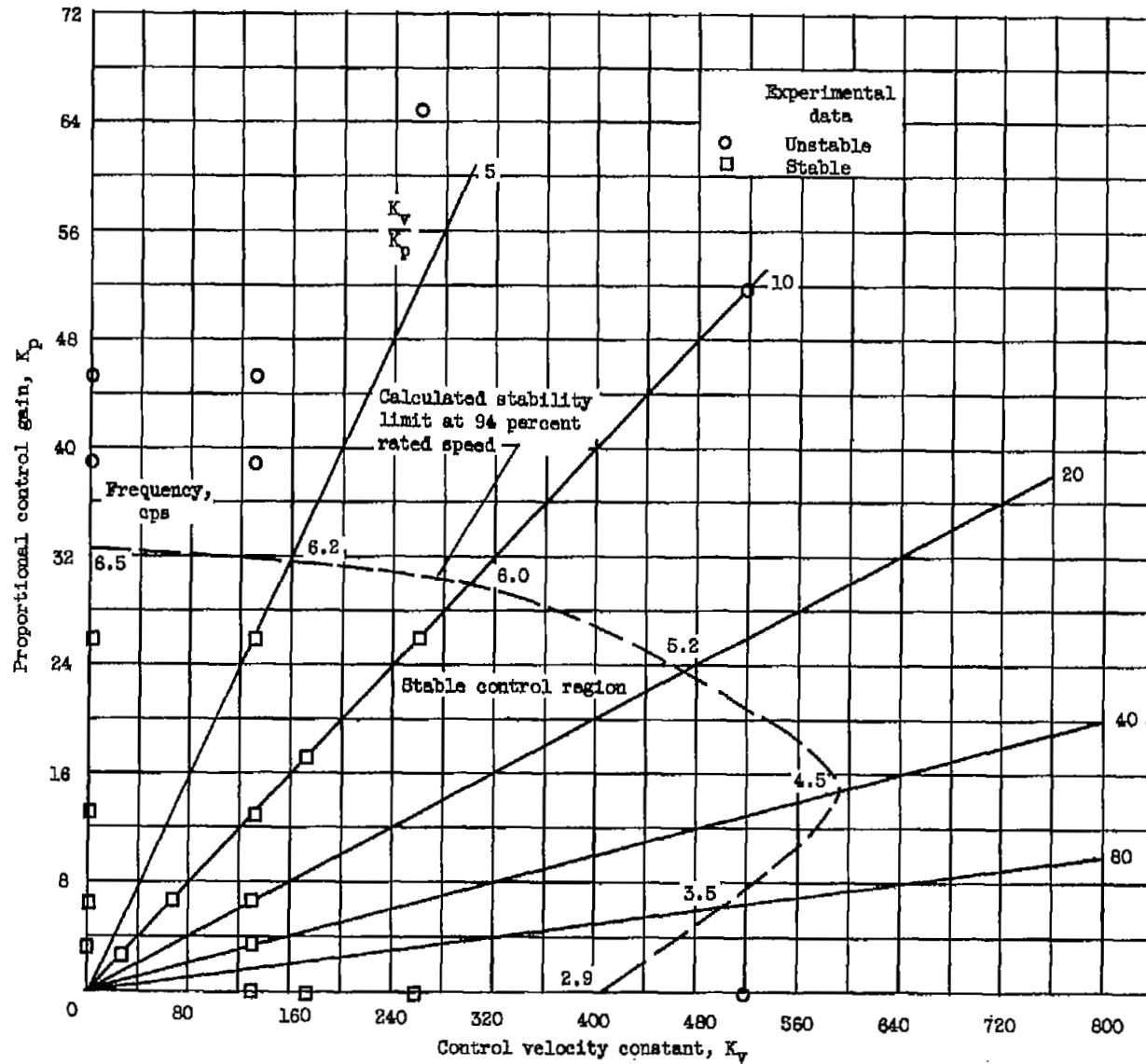
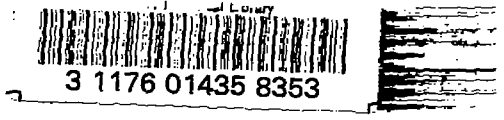
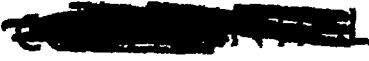


Figure 22. - Stability limit plot for variations of proportional and velocity constant control gain.



2 1 1 2

1

1

1

